COMPUTER SIMULATION OF DEFORMATION BEHAVIOUR OF METALS AT LOW TEMPERATURE

BEING A THESIS PRESENTED

BY

NAEEM FAROOQUI

TO THE
UNIVERSITY OF BALOCHISTAN
QUETTA,

IN APPLICATION FOR

THE DEGREE OF DOCTOR OF PHILOSOPHY

1990

COMPUTER SIMULATION OF DEFORMATION BEHAVIOUR OF METALS AT LOW TEMPERATURE.

BEING A THESIS PRESENTED

BY

NAEEM FAROOQUI

TO THE

UNIVERSITY OF BALOCHISTAN
QUETTA.

IN APPLICATION FOR

THE DEGREE OF DOCTOR OF PHILOSOPHY
1990.

CERTIFICATE

It is a pleasure to certify that this is the bonafide work of Mr. Naeem Farooqui. In my opinion the thesis is suitable for the consideration for Ph.D degree in physics.

(DR. SYED MOHSIN RAZA)
Research Supervisor
and
Chairman
Department of Physics
University of Balochistan
Quetta.

Dedicated to my parents

ACKNOWLEDGEMENT

I express my sincere regards and gratitudes to my supervisor Dr. Syed Mohsin Raza for his guidance, help, encouragement, advices and critics but constructive remarks which made it possible for me to complete the project and prepare Ph.D thesis. Specially being Chairman of Physics Department rendered all possible support and presented my case to the excellence and allowed me to utilise all available facilities of the department to complete my research work.

I also pay sincere tributes and regards to Professor Dr. Abdus Salam who invited me to do research work at Trieste (Italy).

I am also thankful to Prof. Dr. Syed Bande Hassan Abidi ex-Chairman of Physics Department for his cooperation and help in research facilities during his affiliations.

I am grateful, and offer sincere regards to the Vice Chancellor, Member Board of Advanced Studies and administration of the University of Balochistan for granting me all favour, appreciations and maximum support to complete my research work and prepare Ph.D. dissertation.

I shall remain thankful to Mr. Abdul Rauf for typing the manuscript.

My special thanks and blessing go to my parents and family members for their moral support, encouragement and patience.

ABSTRACT

Reviewing the previous theories and models developed for dislocation/dislocations interactions, the relation for the creep rate is modified for low temperatures suggesting that the behaviour of stress relaxation rate is logarithmic in nature. A self-consistent stress relaxation model is discovered for the accurate measurement of activation energy in relaxation rate processes. A single barrier stochastic model of low temperature creep is developed defining dynamic recovery processes; shape of the dislocation is obtained by force balance equation, then using computer model the average dislocation velocity is calculated showing that it never becomes zero. A new force balance equation is used. The dislocations move by forming bulge, and unzipping tendency increases as the strength of the barrier increases contradict Foreman and Makin model (68); the average velocity of dislocations increases with the increase in the size of the array, but for small size the average velocity for each array will be different except where it is constant. Also the dislocations after covering a short distance reach a steady state velocity due to coupling effect between strong and weak barriers. Similarly the dislocation jump approaches an average or steady state velocity after travelling two or three times the insert distances. The deformation on slip plane is controlled by the rate of motion of the pileup nearly equal to the velocity of sound.

However strain enhancement and stress raising in the pre-yield band formation and dynamic recovery occuring at low temperatures show that a multibarrier stochastic model is needed for further studies.

CONTENTS Page No.

CHAPTER 1.

INTRODUCTION

I - CREEP OF SOLIDS AT LOW TEMPERATURES.

II - STOCHASTIC MODEL OF CRYSTAL PLASTICITY.

III - COMPUTER SIMULATION OF LATTICE DEFECTS.

1. INTRODUCTION

I. CREEP OF SOLIDS AT LOW TEMPERATURES:

1.1 EARLY EXPERIMENTAL OBSERVATIONS

In 1930 Meissner, Polanyi and Schmid (1) investigated plastic deformation in metals at liquid helium temperatures. The cadmium single crystals showed a sizable plasticity under deformation at nearly absolute zero, and at stresses several times as high as the yield stress at room temperature. A transient creep stage was revealed on creeping cadmium and a close similarity of the curves at 1.2 and 4.2 was observed. Keeping in view the results given by Meissner and his colleagues(1) in 1956, Glen (2) studied low-temperature creep of cadmium single crystals in detail which gave inadequate quantitative data due to imperfect equipment, but still he managed to gain sound evidence of transient creep varying as lnt.

Then, relation for transient creep in most metals was obtained at low temperatures ($T < 0.2 - 0.3\ T_m$ is the crystal melting temperature) and at very large strains by Wyatt (3) and other workers (4) as:

$$\varepsilon = \alpha \ln(\gamma t+1) \qquad \text{-----(1)}$$

where α and γ are independent of time.

The value of co-efficient α was estimated by Mott (5) theoretically and showed that for thermally activated plastic deformation:

$$\alpha = \frac{kT}{u_o} \Big/ \frac{1}{\sigma} \frac{\partial \sigma}{\partial \varepsilon} \qquad \text{-----(2)}$$

where u_o is the energy of dislocation - impeding barrier,

σ is the applied stress and

$\frac{\partial\sigma}{\partial\varepsilon} = \chi$ is the work - hardening coefficient.

For very simple cases, the activation energy is given by J. Friedel (6) for a dislocation intersection as:

$$\Delta H(\sigma) = U_o - \gamma^* (\sigma - \sigma_i) \qquad \text{----- (3)}$$

where σ_i is the internal stress which is a linear function of deformation and coefficient α, as is represented by A. Seegar, Z. Naturf (7) as:

$$\alpha = kT/kV^* \qquad \text{----- (4)}$$

where V^* is the activation volume and

k is the Boltzman constant.

If work-hardening coefficient at low temperatures is neglected [as from eq.(2) and (4)] then the magnitude of the transient creep is linearly dependent on temperature and tends to zero as $T \to 0K$. However, the experiment or Glen (2) for helium temperatures showed a much larger creep than is given by relation and one which is weak, if at all, dependent on temperature. Since it was unclear what kind of mechanism was responsible for the dependence observed by Glen (2) who assumed that in order to explain the helium temperature creep effects should have been included which were neglected in developing the thermally activated creep theory. Such effects may be dislocation quantum tunnelling barriers and zero-point vibration.

1.2 MOTT'S THEORY OF QUANTUM TUNNELLING BY DISLOCATIONS:

The quantum tunnelling of dislocations through impeding barriers was considered by Mott (8) who estimated the probability of the dislocation slipping through the barrier. A tunnelling dislocation was identified for a particle whose mass is equal to that or the dislocation line element directly interacting with an obstacle. A rectangular barrier was taken as barrier potential. Further, it was proposed by Mott (8) that screw dislocations form barriers when they intersect the crystallographic glide plane of the slipping dislocation. Also, a sessile screw dislocation stops a moving one, which cannot then move further without jogging.

The activation energy for jogging at the stress i.e. for the dislocation to overcome the barrier is given as:

$$\Delta H = \gamma \left(1 - \frac{\sigma}{\sigma_c}\right) \qquad \text{----- (5)}$$

where σ is the applied stress which is smaller than σ_c required to overcome the barrier in the absence of thermal activation. γ is the jog energy.

The best approximation is provided by the relation:

$$\Delta H = W_o \left(1 - \frac{\sigma}{\sigma_c}\right)^{3/2} \qquad \text{----- (6)}$$

where W_o is the value close to the jog energy and equals a few electron volts.

Mott (8) calculated that the probability of barrier tunnelling is proportional to:

$$\omega = \nu \exp\left[-2\alpha_o \left(2MW_o/\hbar^2\right)^{1/2} a\eta\right] \qquad \text{----- (7)}$$

where ν is the atomic frequency of $10^{12}\ s^{-1}$,

M the dislocation effective mass,

α_o the coefficient which is unity,

a is of the order of magnitude of the inter-atomic seperation,

and $\eta = 1 - \sigma/\sigma_c$

We observe that the dislocation velocity is directly proportional to the probability of the dislocation passing through the barrier. Thus, in case of quantum tunnelling through barriers the dislocation velocity is independent of temperature.

The temperature above which thermal fluctuations prevail as the mechanism of over coming barriers can be found by comparing the probabilities of the two processes. For thermally activated dislocation motion, it is assumed that:

$$\omega = \nu \exp\left(-W_o \eta^{3/2} / kT\right) \qquad \text{----- (8)}$$

We derive that thermally activated overcoming of barriers which is dominant provided that:

$$\frac{W_o \eta^{1/2}}{kT} > 2 \left(\frac{2MW_o}{h^2}\right)^{1/2} a \qquad \text{----- (9)}$$

By transformation process and eliminating η, Mott (8) arrived at an expression to obtain the temperature at which both the processes are equally probable: i.e.

$$\frac{kT}{W_o} \sim \left(\frac{m_o}{M}\right)^{3/2} \left(\frac{1}{2}\right)^{3/2} (30)^{1/2} \qquad \text{----- (10)}$$

where m_o is the electron mass.

If we agree with Mott (8), $m_o/M \simeq 0.5 \times 10^{-5}$ and $W_o \sim 1.6 \times 10^{-16}$j (1 eV), then T ≃ 1K.

Thus, the creep depends on dislocation quantum tunnelling at T < 1K and on thermally activated processes at T > 1K. Here, the critical temperature derived is an estimate, which may depart from the exact value by several times for different approximations while calculating, the theory nevertheless yields the important result that creep controlled by quantum tunnelling does not depend on temperature.

Mott's (8) theory allows to estimate a creep deformation given by equation $\varepsilon = \alpha \ln (\gamma t)$, where α is independent of temperature and is given by:

$$\alpha = \text{constant} / a \left(2MW_o / \hbar\right)^{1/2} \qquad \text{----- (11)}$$

where constant is unity.

Then calculations of the creep deformation increment between times t_1 and t_2;

$$\varepsilon_2 - \varepsilon_1 = \alpha \ln \left(t_2 / t_1\right) \qquad \text{----- (12)}$$

leads to a value which can be compared with the experimental result within the order of magnitude.

Nabarro (9) reviewed Mott's model of low temperature creep and proposed some modifications. However, even with these modifications Nabarro found that Mott's estimate of the temperature below which tunnelling of dislocations through barriers could occur (≃ 1K) was confirmed.

1.3 DISLOCATION QUANTUM TUNNELLING THROUGH PEIERL'S BARRIER:

In continuation of the observation Leibfried (10) analyzed the quantum motion of the dislocation segment with its end pinned by local defects and observed quite high dynamic forces exerted on the defects by the zero point vibrations of the segment at T=0. Then Weertman (11) gave a proposal of quantum - induced double kinking in a dislocation moving across the Peierls potential relief. Later Alefeld (12) and Gilman (13) studied other aspects of the same problem treating simple models, so their results are no more than tentative qualitative estimates of the action of quantum effects on dislocation mobility. A more rigorous formulation of the problem of the quantum effects of a dislocation across the Peierls relief was solved by Petukhov and Pokrovskii (14) and the quantum mechanisms of the overcoming of local barriers were analyzed by Natsik (15, 16). We now proceed with their results.

We start with a mechanical model of dislocation as a flexible elastic string with linear mass density m and linear energy density C (tension coefficient). Suppose that the dislocation travel in the slip plane in a uniform field of external stresses and a potential barrier field. Then the instantaneous dislocation configuration is described by the function u(x,t), where u is the cartesian coordinate of the dislocation line elements along the direction of dislocation movement, x is the transverse coordinate and t,the time. The ends of the dislocation line are thought of as fixed and aligned, so that;

$u(\infty,t) = u(-\infty,t) = 0$. The string Hamiltonian is as:

$$H = \int_{-\infty}^{+\infty} dx \left[\frac{1}{2} m \left(\frac{\partial u}{\partial t}\right)^2 + \frac{1}{2} c \left(\frac{\partial u}{\partial x}\right)^2 + U(u,x) - b\sigma u \right] \quad \text{---- (13)}$$

where the first and second summands under the integral shows the linear densities of the kinetic and potential energies of the bent string. U(u,x) and $b\sigma u$ are the potential energy and linear density in the barrier field and in the applied stress field, and also U(u,x) depends on the barrier shape.

For the Peierls barrier it is a function of a single variable, the displacement u: $U(u,x) = U_p(u)$, where $U_p(u)$ is a periodic function with the period equal to the lattice parameter a along the direction of slip. For barriers associated with local defects, the potential U(u,x) depends on both the variables which is nonzero close to the defect, in a region measuring d~a. But for semi-quantitative theory we need not distinguish between the magnitudes of a and b.

In crystals with high Peierls barriers, dislocation move by the development and widening of double kinks. At high temperature this is due to thermal fluctuations, but at very low temperatures thermal fluctuation is replaced by temperature-independent quantum effects as the mechanism of overcoming barriers.

As shown in Fig.(1) the dislocation is taken to be an elastic string in a plane potential relief $\phi(u)$ made up by the periodic potential (Peierls) and the linear term $b\sigma u$ due to the applied stress σ given as:

$$\phi_\sigma(u) = u_p(u) - b\sigma u \quad \text{---- (14)}$$

represented in Fig.(2) is considered. In simple form the problem is to obtain a path from the metastable equilibrium with u=0,the stable equilibrium with u=a.

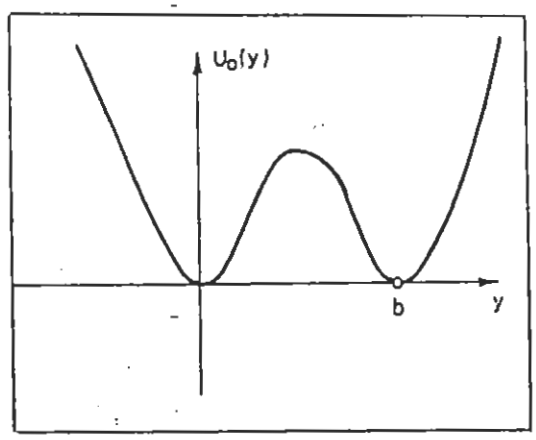

Fig. 2. Two neighbouring minima (valleys) in the Peierls relief.

Here the problem is more concerned, but for the two limiting cases viz; that for the applied stress σ much lower than the Peierls stress σ_p ($\sigma << \sigma_p$) and that of the near-Peierls external stress ($\sigma \lesssim \sigma_p$), it can be solved in true value. Further when $\sigma > \sigma_p$ the minima in the potential $\phi(u)$ vanishes and then the dislocation is controlled by dynamic mechanisms, while at $\sigma < \sigma_p$the dislocation is initially present in one of the valleys of the relief u=0, but due to thermal or quantum fluctuations, the dislocation moves to the neighbouring minimum with u=a.

The probability of the quantum transition ω_q, having the total string energy E, may be calculated in the quasi-classical approximation by the Feynman relation (17).

$$\omega_q(E) \propto \exp\left(-\frac{2}{\hbar}(J_m S_E)_{min}\right) \quad \text{--------} \quad (16)$$

where $(J_m\ S_E)_{min}$ is the minimum value of the imaginary part of the mechanical action along trajectories in the space of configuration with u(x) coming from "point" u=0 to "point" u=a.

For small stresses $\sigma << \sigma_p$ the minimum-action trajectory runs through the top point $U_c(x)$ corresponding to the double-kink configuration as in Fig(3) known from the theory of thermally activated dislocation motion in Peierls relief (18,19).

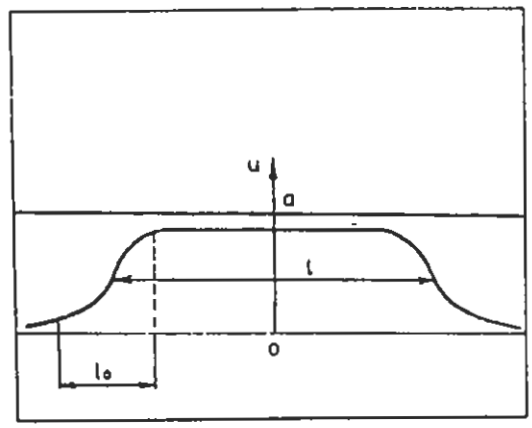

Fig. 3. Double kink in a dislocation: l is the double-kink length, l_0 the single-kink width [13].

The function S(E) is obtained from Hamilton-Jacobi relation, i.e. if the total energy E is smaller than U_c, then the total potential energy of the string is the critical configuration corresponding to the top point; then the originating and widening of a double kink proceed by quantum tunnelling through the Peierls barrier. The probability of such process is given as:

$$\omega_q\ (\sigma;\ T) \sim \exp\ \left(\frac{-4(2M)^{1/2} U_c^{3/2}}{3\hbar\ b^2\ \sigma}\right);\quad T < T_o \qquad \text{---- (17)}$$

$$\omega_q(\sigma,T) \sim \exp\left(\frac{-U_c}{kT} + \frac{\hbar^2 b^4 \sigma}{24M(kT)^3}\right) \quad T > T_o \quad \text{--- (18)}$$

where;

$$T_o = \hbar\, b^2\sigma \,/\, 2(MU_c)^{1/2} \quad \text{--- (19)}$$

and

$M = mb^2/2l_o$, where l_o is the unit kink length.

When the double kink passes the barrier then it loses its stability and, by widening, brings the dislocation to the minimum u=a. For $T < T_o$, the probability is entirely controlled by the quantum properties of the dislocation and is independent of temperature. In order to obtain $\ln\omega$ in this case recourse can be made to the Guyot and Dorn calculation (18) of V_1 which gives:

$$\ln\omega \simeq -\frac{a}{\hbar}\left(G\, b^3 M\right)^{1/2} \frac{\sigma_p}{\sigma} \quad \text{---- (20)}$$

where $\frac{\sigma_p}{\sigma}$ characterizes the amplitude of the zero-point vibrations. As such, quantum effects are expected to occur in materials featuring zero-point vibration amplitudes which are not very low.

At $T \simeq T_o$, the most likely transition is a complex process in which thermal activation is followed by tunnelling. Its probability equals the product of the probabilities as:

$$\omega \sim \exp\left(\frac{-\alpha U_c}{kT} + \frac{1}{24} - \frac{G^2 b^2 \hbar^2}{mT^3}\right) \quad \text{---- (21)}$$

Here we consider two cases:

At high temperatures $T >> T_o$, the probability of the transition assumes the usual form for classical thermally activated motion; and secondly when $\sigma_p - \sigma << \sigma_p$ for low

temperature $T << T_o$, then the overcoming of the Peierls barrier by the dislocation is given in terms of tunnelling effect so that transition probability is:

$$\omega(\sigma,0) \sim \exp\left(\frac{-2S_o b(cm)^{1/2}(\sigma_p-\sigma)}{\hbar\beta}\right) \quad \text{---- (22)}$$

Where S_o depends on the type of the barrier

and $$\beta = \frac{1}{6}\left(\partial^3 U_p/\partial u^3\right)_{u=0}$$

In both cases, the probability of tunnelling-induced development of a double kink increases with the external stress σ. While at high temperature $T >> T_o$, a usual activation dependence for the transition probability is achieved:

$$T_o \approx \frac{\hbar}{\pi m}\left[b\beta(\sigma_p-\sigma)\right]^{1/4} \quad \text{---- (23)}$$

The temperature T_o which is responsible for dividing quantum and thermally activated dislocation motion depends both on the barrier dislocation parameters and on the stress σ. As such to have a clear picture of T_o, it will be preferred to express it in terms of the Debye temperature of the crystal, T_D given as:

$$T_o(\sigma) = \begin{cases} 10^{-1}\,\frac{\sigma}{G}\,T_D & ; \quad \sigma << \sigma_p \\ 10^{-1}\left(\frac{\sigma_p}{G}\right)^{1/2}\left(1-\frac{\sigma}{\sigma_p}\right)^{1/4} & ; \sigma_p - \sigma << \sigma_p \end{cases} \quad \text{----(24)}$$

So T_o may occur in the range about 1K, which is now available, only for crystals with high Debye temperature and high Peierls barrier.

It is possible to obtain dislocation velocity while overcoming the Peierls relief by relations derived for the

transition probability. The calculated value gives probability of double kink nucleation per unit time and per unit length, shown by R and velocity of kink spreading by v. It is observed that the time taken for the dislocation transition to the next valley is 1/R. If the dislocation length is great enough for a number of double kink nucleations to occur, then the nucleation of double kinks, their spreading and annihilation on meeting will be responsible for the dislocation transition to the next valley, such that the corresponding equations lead to the expression for the transition time $t \sim (VR)^{-1/2}$. In general, second case is observed. So rate of deformation due to motion of dislocation through a crystal with high Peierls barrier can easily be calculated.

1.4 QUANTUM DISLOCATION MOTION THROUGH LOCAL BARRIERS:

In some crystals, Peierls barriers in easy glide planes are small and so dislocation mobility is determined in terms of its interaction with local defects so that $\alpha > \sigma_p$, i.e. dislocation motion is entirely controlled by the overcoming of local defects, neglecting Peierls barriers. Natsik (15,16) solved this effect in terms of quantum mechanics.

As in Fig.(4), consider a dislocation segment driven by a stress $\sigma_p < \sigma < \sigma_c$ which is stopped by local defects A, O and B.

For the analysis of the passage of dislocation over the central defect O, we ignore the possible unpinning from the A to B defects taken as point obstacles so that dislocation pinning at these defects is rigid. The problem is to calculate

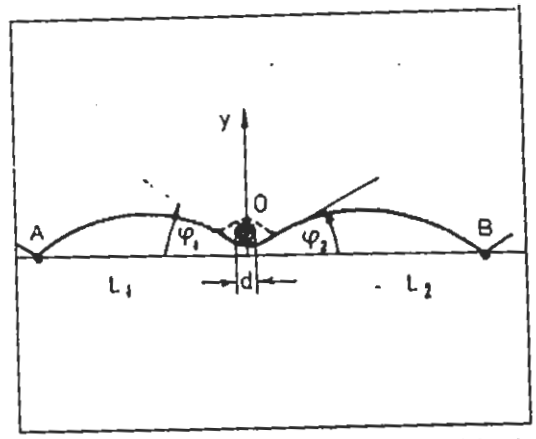

Fig. 4. Motion of a dislocation segment AB in the potential field of a defect 0: d is the size of the defect and of the central dislocation segment; L_1 and L_2 the left and right segment lengths; φ_1 and φ_2 the instantaneous values of the angles of attack for the left and right segments; y the coordinate of the central dislocation element [15].

the probability of transition from the metastable configuration "before the defect" shown by solid lines to the configuration "after the defect" shown by dashed line. Also it is known that potential U(u,x) possesses double character so the problem if solved by previous method then the dislocation transition through the Peierls barrier gives unsurmounted difficulties. As such Natsik made very simple assumptions which permitted him to solve the problem keeping its vital features unchanged. The interaction with the defect involves no more than a microscopic dislocation element d in length and not the entire dislocation, then segments L_1 and L_2 adjacent on both sides to this element behaves as strings with the ends localized at the defects. So, the former system is divided into two sub-systems; the central element d and the two sgements L_1 and L_2 neglecting the interaction between the later. The interaction between the central element and the dislocation segments is realized by the line

tension.

This is justified, if the motion of the central element is considered within an area comparable with the defect size and restrict the description of the motion of the segments L_1 and L_2 to the long-wave vibrations with the mimimum wavelength $\lambda > d$. In this case, the most important aspect is to choose the proper relation giving the energy of interaction between the above sub-systems. For qualitative result for this interaction, Natsik used expression obtained by Granato and Lucke (20) and Leibfried (10). They assumed that the defect is sufficiently "strong" i.e. the self energy cd of the dislocation element directly interacting with the defect is much lower than the maximum energy of the interaction U_o. This is called strong coupling condition written as:

$$z = \left(cd/U_o\right)^{1/2} < 1 \qquad \text{---- (25)}$$

The system Hamiltonian can be written due to assumptions which includes the energies of both sub-systems and the energy of interaction between them. So shifting from classical Hamiltonian to the quantum and sloving the schrodinger equation, the wave function is obtained. We calculated the probability of the transition of the dislocation central element from the area "before the defect" to the area "after the defect". The average transition frequency is:

$$\omega = \nu \exp\left[-S\left(1-\frac{\sigma}{\sigma_c}\,;\ T\right)\right] \qquad \text{---- (26)}$$

Where S is a non-negative function of stress and temperature having a non-zero value at T=0 and tends to zero at $\sigma=\sigma_c$, where σ_c is the critical dislocation umpinning stress,

i.e. the stress at which a dislocation unpins by a purely mechanical technique without fluctuations. The function S depends on the shape of the barrier provided by the defect.

For high, narrow barriers:

$$S\left(1-\frac{\sigma}{\sigma_c};T\right) = B_o\left(1-\frac{\sigma}{\sigma_c}\right)^{5/4} - \frac{25}{64} B_1\left(1-\frac{\sigma}{\sigma_c}\right)^{1/2}\left(1+\frac{T^2}{\theta^2}\right) \quad --(27)$$

whereas for low, broad barriers:

$$S\left(1-\frac{\sigma}{\sigma_c};T\right) = \frac{E_o\left(1-\frac{\sigma}{\sigma_c}\right)^2}{kT^*(T)} \quad --- (28)$$

where constants B_o, B_1 and E_o are determined by barrier and dislocation parameters:

$$B_o \sim \P d \left(Mv_o\right)^{1/2}/\hbar \; ; \; B_1 \sim ZB_o \; ; \; E_o \sim \lambda U_o^2/\theta cd^2 \quad ---(29)$$

Where θ is the characteristic dislocation temperature estimated as a certain proportion of the Debye temperature of the crystal, T_D:

$$\theta = \frac{\P\hbar}{2\lambda}\left(\frac{c}{M}\right)^{1/2} \simeq \frac{1}{3}\left(\frac{1}{\lambda}\right)T_D \quad --- (30)$$

Since λ should be of the order of a few atomic sizes, then θ may be roughly estimated as $\theta \simeq T_D/10$. θ is most essential characteristic of the quantum overcoming of barriers. At temperatures $T \lesssim \theta$, quantum effects become essentially important.

The dislocations are observed to overcome a barrier mainly by tunnelling of the crystal element d through the potential hill for high, narrow barriers. This is shown by Mott (8). But Natsik relation is different from Mott's. According to Natsik, the probability of a dislocation tunnelling

through a barrier is a weak function of temperature (the second summand of eq.27). This is due to motion of segments L_1 and L_2, which slightly increases the probability. Mott ignored temperature dependence property. In this case, switching to the usual thermal activation expression takes place at the temperature:

$$T_o \sim \frac{2U_o}{k} \left(1- \frac{\sigma}{\sigma_c}\right)^{3/2} \qquad \text{----- (31)}$$

Similarly, for wide and low barriers, the probability of the tunnel effect becomes small, and the overcoming of the defect by the central element d is obtained by quantum motion i.e zero-point vibrations and thermal motion of the segments L_1 and L_2. Further in eq.(28) for this case, there appears the quantity T^*, the effective temperature, depending on temperature T and taking on the value:

$$T^* = \begin{cases} \frac{\theta}{2} \left(1+ \frac{T^2}{\theta^2} \right) & \text{for } T < \theta \\ T & \text{for } T > \theta \end{cases} \qquad \text{----- (32)}$$

Thus eq.(26) for the average frequency of transition through the defect becomes:

$$\omega = \nu \exp \left[-E_o \left(1- \frac{\sigma}{\sigma_c}\right)^2 \Big/ kT^* \right] \qquad \text{----- (33)}$$

but for temperatures above θ the relation gets the usual form for the classical thermally activated process:

$$\omega = \nu \exp \left[-E_o \left(1- \frac{\sigma}{\sigma_c}\right)^2 \Big/ kT \right] \qquad \text{---- (34)}$$

Thus, θ represents the temperature above which thermally activated processes prevail, and below which quantum processes are dominant. The above estimates give that the influence of quantum effects on the overcoming of local barriers by

fluctuations may be observed at temperatures of several tens of degrees.

These two cases considered give that the probability of dislocation movement through a barrier has a non-zero value as $T \to 0K$, which is the consequence of the quantum properties of the dislocation. But in the second case, the dislocation motion through the defect as $T \to 0K$ is due to dynamical lowering of the barrier as a result of zero-point vibrations of segments L_1 and L_2. At $T > 0K$, thermal motion is superimposed on quantum motion and the probability of the transition through the barrier becomes temperature dependent. However, this dependence remains weak until many dislocation vibrational modes are excited.

Natsik's theory and the ensuing formulae permit a comparison with the experimental dependence. An analysis of the experimental data showed that they are best described by the relations for the second limiting case. Therefore, in writing the equations for the kinetics of plastic deformation, we shall use eq.(26). The rate of plastic deformation may be written as:

$$\frac{d}{dt}\,\varepsilon = \nu\varepsilon_o \exp\left[-S\left(1-\frac{\sigma - \sigma_i^{(0)} - \kappa\varepsilon}{\sigma_c}\,;\,T\right)\right] \qquad \text{--- (35)}$$

where σ denotes an average stress in the crystal due to external crystal - deforming forces, and $\sigma_i^{(0)}$ the internal stresses at the starting moment of deformation and κ the work-hardening co-efficient.

The internal stresses are assumed in this analysis to be directly proportional to the deformation. The effective

stress acting on the dislocation is then given as:

$$\sigma^* = \sigma - \left(\sigma_i^{(0)} + \kappa\varepsilon\right) \qquad \text{---- (36)}$$

Integration of eq.(35) for σ = constant (creep) leads to the logarithmic creep law:

$$\varepsilon(t) = \alpha \ln\left(\gamma t + 1\right) \qquad \text{----- (37)}$$

where;

$$\alpha^{-1} = \kappa \frac{\partial}{\partial \sigma^*}\left[\bar{S}\left(1 - \frac{\sigma^*}{\sigma_c}\,;\, T\right)\right] \qquad \text{---- (38)}$$

and

$$\gamma = \alpha^{-1}\,\varepsilon_o \nu \exp\left[-S\left(1 - \frac{\sigma^*}{\sigma_c}\,;\, T\right)\right] \qquad \text{---- (39)}$$

For the second case; where S is defined by eq. (28):

$$\alpha = \frac{kT^*}{\kappa v^*} = \frac{k\theta}{2\kappa v^*}\left(1 + \frac{T^2}{\theta^2}\right) \qquad \text{---- (40)}$$

where

$v^*(\sigma^*) = \left(E_o/\sigma_c\right)\left(1 - \frac{\sigma^*}{\sigma_c}\right)$ is the activation volume.

II. STOCHASTIC MODEL OF CRYSTAL PLASTICITY:

The use of statistical methods to account for heterogeneity of the microstructure of crystalline materials in creep theories was observed before then Taubert (21) who reviewed the work and suggested several creep laws of crystalline solids were a consequence of basic stochastic features of the kinetics of dislocation ensembles. It was then used by Feltham (22) to develop a model, the results of which are used in the present case where the transition of slip unit occurs as in Fig.(5).

This change is from barrier u_j to another with the

Mathematically defined as:

$$\frac{\partial n}{\partial t} = D \frac{\partial^2 \left[n \exp\ (-u/kT) \right]}{\partial u^2} \qquad \text{-------- (41)}$$

where;

$$D = \frac{1}{2} \nu\ (\delta u)^2 \qquad \text{-------- (42)}$$

where; ν is the atomic frequency,

but; $N\ (u,t) = n(u,t)\ \exp\ (-u/kT)$

then eq.(41) becomes:

$$\frac{\partial N}{\partial t} = D \exp\ (-u/kT) \frac{\partial^2 N}{\partial u^2} \qquad \text{------ (43)}$$

eq. (43) is Fokker-Planck relation of an Ornstein - Uhlenbeck process in the stochastic variable N (24). If the distribution N(u,t) is obtained and area A^* is taken to be constant during isothermal creep, then creep rate in shear is:

$$\dot{\gamma} = \nu b A^* \int_u N du \qquad \text{------ (44)}$$

such that; $u_1 \leqslant u \leqslant u_2$ ------ (45)

The upper limit is taken to be ∞ while $u=u_1$, yet not invalidate solutions of N obtained without restriction on the range of u-values, if the net influx or outflux from the u_1 link were replaced by the action of source or sink of dislocations. But logarithmic type of creep dislocations are generated at very early stages.

Therefore, the solutions of eqs. (42) and (43) remain valid over the range $u_1 \leqslant u$ while for $u < u_1$ the set is empty; i.e. $n(u) = 0$.

However, it has been observed that if creep is

observable , then a value u^* is selected such that:

$$u^* = \frac{1}{2}(u_1 + u_2) \qquad \text{-------} \quad (46)$$

and characteristic retardation time given as:

$$t^* = \left(\frac{1}{\nu_D}\right) \exp\left(\frac{u^*}{kT}\right) \qquad \text{-------} \quad (47)$$

where ν_D is an atomic frequency equal to $D/(kT)^2$. If however the quantity δu as in eq.(42) is taken to be of the order of a tenth of electron volt, then at T = 0k, ν_D and ν in eq.(44) will be equal to about 10^{10}/sec.

Then, if 't' equals to a few seconds then;

$$u^* = mkT \; ; \quad m \simeq 25 \qquad \text{-------} \quad (48)$$

These results have been verified on magnesium crystals deformed between 4.2 and 420 k by Conrad et al, Sharp and Christian (25).

2.1 LOGARITHMIC CREEP:

Although S-shaped creep curves have been observed and can be explained in terms of a solution of eqs.(43) and (44) i.e. by Bekirovic et al (26), the commonly observed form of creep at relatively low temperatures is logarithmic (27).

Eq.(43) in this case has the solution:

$$N(u,t) = N^* \frac{\phi(u, t + t_o)}{(t+t_o)/et^*} \qquad \text{------} \quad (49)$$

Where N^* and t_o are constants and e is the base of natural logarithms.

The function ϕ is given by:

$$\phi = \exp\left(-\frac{\exp(u/kT)}{\nu_D\,(t+t_o)}\right) \qquad \text{------ (50)}$$

However, a non-zero value of t_o in eq. (49) proves the existence of u-spectrum at the onset of creep.

Here if area A^* is written as:

$A^* = l^*\,(rb)$

where l^* is the most probable segment length.

and rb a length in terms of the modulus of Burgers vector b.

Now, replacing N^* by $n^* \exp(-u^*/kT)$, in accord with the transformation leading to eq.(43), (44) and (49) yield:

$$\dot{\gamma} = \dot{\gamma}_o \left(1 + \frac{t}{t_o}\right)^{-1} \int_{\Delta u} \phi\, d\,(u/kT) \qquad \text{----- (51)}$$

$$\text{where} \quad \Delta u = u_2 - u_1 \qquad \text{----- (52)}$$

but $$\dot{\gamma}_o = \nu\, rb^2\, \rho \left(\frac{t^*}{et_o}\right)\left(\frac{kT}{\Delta u}\right) \exp\left(\frac{-u^*}{kT}\right) \qquad \text{---- (53)}$$

$$\text{and} \quad \rho = l^*\, n^*\, \Delta u \qquad \text{------ (54)}$$

which gives the density of all dislocations migrating over barrier in the physically realized barrier-height range Δu.

Here eq.(51) shows that were it not the time dependence then it would represent logarithmic creep.

It is clear from eq.(50) that for any 't' the value of 'ϕ' will be close to zero for all u-values greater than about $kT \ln\left[\nu_D\,(t + t_o)\right]$ for these the integrand in eq.(51) is zero; for others ϕ will be one, so the integral in eq.(51) is equal to $\ln\left[\nu_D\,(t + t_o)\right]$.

Substitution of values in eq.(51), γ can be obtained yielding a creep relation of lesser curvature, which is similar to observations of Wyatt (27). So eq. (49) gives logarithmic creep.

The creep rate is given as:

$$\dot{\gamma} = \frac{\alpha}{1+t/t_o} \qquad \text{----- (55)}$$

The determination of the stress dependence of α, from eq.(53) is difficult without assumptions.

The single barrier Model of logarithmic stress-relaxation Feltham (28) and thus also of logarithmic creep with which it can be associated Rohde and Nordstrom (29) leads to a linear dependence of α on the applied stress.

2.2 THEORETICAL MODEL OF THE CREEP PROCESS:

In case of crystal plasticity (30) distribution of heights of energy barriers to dislocation movement and rearrangement ability of dislocations minimizing the elastic potential of the material are considered.

This tendency manifests itself resulting in the formation of dipoles, multipoles and barriers of the Cottrell-Lomer type (31).

The occurrence and interrelation of recovery and work-hardening, specifically in creep has been seen by the conversion of long-range stress-fields to shorter-range ones.

The model described is taken to be adequate for restricted modes of dynamic recovery operative in the absence of diffusion.

Describing the rate process for the case where the

number of barriers of effective height u per unit volume is $n(u,t)$. δu at 't'.

so;

$$\frac{\partial n(u,t)}{\partial t} = \nu \left[n(u,t) \left(\frac{-u}{kT} \right) - n(u-\delta u, t) \exp \left(\frac{-u-\delta u}{kT} \right) \right] \quad --(56)$$

or;

$$\frac{\partial n}{\partial t} = (\nu \delta u) \frac{\partial (n \exp - u/kT)}{\partial u} \quad ---(57)$$

where ν is the Debye frequency using transition probability (32):

$$N(u,t) = n(u,t) \exp(-u/kT) \quad ---- (58)$$

eq. (57) becomes:

$$\frac{\partial N}{\partial t} = (\nu \delta u) \exp(-u/kT) \frac{\partial N}{\partial u} \quad ---- (59)$$

then the integral will give the whole value over the u-spectrum (32).

Introducing a variable $r = \exp(u/kT)$

so; $dr = (r/kT)\, du$

put in eq.(59);

$$\frac{\partial N(r,t)}{\partial t} = D \frac{\partial N(r,t)}{\partial r}$$

where ; $D = \nu (\delta u/kT)$ ---- (60)

giving solution in the form:

$$N = \phi (r+Dt) \quad ---- (61)$$

For initial condition; eq.(58) implies that:

$$N(u,0) \propto \exp(-u/kT) = \frac{1}{r} \quad ---- (62)$$

which satisfies the condition;

$$n(u,0) = \text{constant}, \; u_1 \leqslant u \leqslant u_2 \quad ---- (63)$$

$$\text{if } N \propto (r + Dt)^{-1} \quad ---- (64)$$

Under these conditions for creep the other possible approximations will not influence these results. It can be further shown that the integration of eq.(64) over the u-spectrum as by (63) gives strain rate as:

$$\dot{\varepsilon} \propto \frac{1}{t} \ln\left[\frac{1 + Dt \exp\left(-u_1/kT\right)}{1 + Dt \exp\left(-u_2/kT\right)}\right] \qquad \text{--- (65)}$$

Here the constant of probability can be evaluated easily. Now there are two special cases which are of importance.

Firstly, if $Dt \exp\left(-u_2/kT\right) >> 1$, then it is known that $u_2 > u_1$ the logarithmic term as in eq. (65) is nearly equal to $(u_2-u_1)/kT$, defining only logarithmic creep.

Secondly, if $Dt \exp(-u_1/kT) << 1$, then again the logarithmic term in eq. (65) becomes equal to $Dt \exp\left[\left(-u_1/kT\right) - \exp\left(-u_2/kT\right)\right]$; showing the creep rate be constant or time-independent.

III. COMPUTER SIMULATION OF LATTICE DEFECTS:

We used the computer as a simulator - that is as a device for setting up a readily tested model of a system under study. Simulation implies the assembling of physical components in such a way that the behaviour of the assembled system can be directly related to that of the original system. Physical testing such as the stochastic model, stress relaxation model and self-consistent stress relaxation model can be regarded as a normal simulation in which case experimental results are tested.

The method of simulation makes use of the computer to

establish the model. We studied the dislocation behaviour at low temperatures using numerical testing and computer simulation techniques. Simulation is perhaps a way of thinking it lends itself to think about a system in terms of transfer-function blocks and basic relationship among variables. Our analysis employ parametric simulation of deformation behaviour of metals at low temperatures rather than testing stochostic models itself.

Later, the computer simulation techniques were successfully applied to many of the experiments by workers entrusted in this field.

Some of the work done is categorily described and reviewed here:

The potential functions and the simulation of defects in lattice dynamical defect problems were studied by Maraudin(33) which revealed that the use of potential functions in these problems differ from their use in other types of problems in crystal physics.

Then later Weiner et al (34) studied computer simulation of quantum phenomena which was the particle method for the solution of the time-dependent schrodinger equation choosing dependent variables leading to the hydrodynamic analogy to quantum mechanics and this method is close in spirit to computation techniques for classical mechanics.

Next, the pseudopotential calculation of point defect properties in simple metals were observed by HO (35) who calculated the vacancy formation energy and formation volume for alkali metals and aluminium crystals.

This work was then extended by Chang (36). He observed that the second-order perturbation pseudopotential calculation may break down on account of strong localized distortion near the point defect.

Later, dislocations and stacking faults were observed and different workers studied their effects by using simulation techniques. The influence of dislocations on electron microscope crystal lattice images were undertaken by Parsons (37). Then on the motion of the $\frac{a}{2} < 111 >$ screw dislocation in models of α-iron was defined by Gehlen (38).

Later, the factors controlling the structure of the dislocation cores in BCC crystals was studied by Vitek et al (39).

The extended defects in copper and their interactions with point defects were described by Perrin et al (40). The partial dislocation interactions in a face-centered cubic sodium lattice were studied by Basinski et al (41), who then described the motion of screw dislocations in a model BCC sodium Lattice (42).

Tyson (43) gave atomistic calculations of Peierls-Nabarro stress in a planar square Lattice; all of the above cases however followed parametric analysis through simulation techniques.

Various studies on surfaces and interfaces and simulation on surfaces by the simulation of pairwise interactomic potentials were made (44). Wette (45) studied the calculations of dynamical surface properties of crystals on computer. The studies were exhausted by Dahl et al (46) by giving a computer

simulation study of grain boundaries in FCC Gamma-iron and their interactions with point defects and Weins (47) obtained computer simulation of the structure of high angle grain boundaries.

Now considering the study of defects in crystalline solid, following are the fields where computer simulation has proved valuable:

a) Fast neutron cascade and ion penetration studies.
b) Shock waves in crystalline solids.
c) Thermal motion and atom transport.
d) Static defects-their atomic configurations, self and interaction energies.
e) Computer simulation of electron microscope diffraction contrast defect images.

All these fields require distinct simulation procedures, however the most useful is the case of static defect which was studied by Bullough and Perrin (48) and Perrin, Englert and Bullough (49) who discussed the aggregation of interstitials in a body-centred cubic lattice. They also studied using simulation procedures the point and line defects in a face-centred cubit lattice. Nevertheless, no such simulation techniques has ever been applied to our case study.

In our study of simulation of deformation behaviour of metals, we took help from NAG (Numerical algorithm Group) FORTRAN Library and used routine structures on VAX-11/730-UMS and VAX-11/780-UNIX mainframe computers both at ICTP (Trieste, Italy) and at physics department of the University of Balochistan.

We used in our simulation studies the following routine structures from NAG Library i.e;

- Monte-Carlo method (D01GBF, D01FBF).
- Runge-Kutta-Merson method (D02PAF, D02QAF, D02QDF*, D02YAF).
- Pseudo-random generators (G05CAF, G05DAF, G05DGF, G05DYF).

The help in retrieving the routine structures were mostly observed through Dr. Carr (Trieste, Italy). Analytical treatment of the problem was studied in physics department.

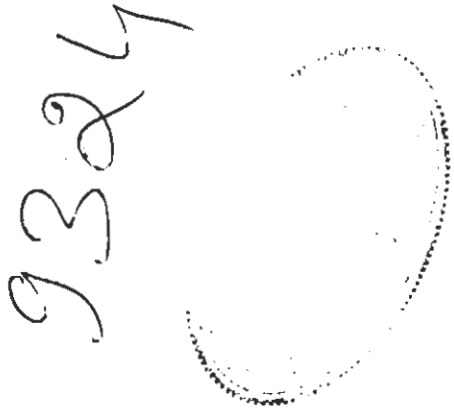

CHAPTER 2.

RESULTS AND DISCUSSIONS

A - STOCHASTIC MODEL OF LOW TEMPERATURE CREEP AND STRESS RELAXATION IN SOLIDS

B - COMPUTER SIMULATION OF DISLOCATION MOTION

A. STOCHASTIC MODEL OF LOW TEMPERATURE CREEP AND STRESS RELAXATION IN SOLIDS:

Dislocations tend to regroup themselves in the course of creep under the influence of forces resulting from mutual interactions thus causing a reduction in the elastic potential associated with the heterogeneous interval stress field. Spatial and temporal fluctuations of internal stresses in describing dislocation glide and other slip processes in solids have attained significant interests in recent years presumably due to availability of computers and sophisticated techniques in numerical analysis. This is why we considered computer simulation studies of dislocation motion as part B of our results and discussions, preferably from the view point of the concept of localised stress relaxation. However, we have restricted our studies to very simple cases for computer simulation of dislocation motion.

In accord with concept of localised stress relaxation, we developed a model (50) for low temperature i.e. when diffusional forms of recovery are in-operative; and which allows activated jumps of a given slip unit only to lower energy barriers.

STOCHASTIC MODEL OF LOW-TEMPERATURE CREEP:

We considered high-temperature creep model of Feltham (51) and allowed structural heterogeniety of the material in terms of a dispersion of heights of energy barriers controlling the stress induced movement of dislocations. A partial analysis of low-temperature creep with particular reference to

experimentally observed logarithmic creep of aluminium and copper has already been made by Buckle and Feltham (52). Our stochastic model of low-temperature creep yields logarithmic $t^{1/3}$-type and other creep functions commonly observed.

We consider constant creep-stress to the specimen. Stress will cause mechanically unstable grouping either of dislocations or of other slip units, within the heterogeneous stress field. Let us consider two dislocations (say edge,) of opposite signs, lying on parallel slip planes; they are denoted by "a" and "b". Both of these dislocations are assumed to to be subjected to a drag force due to energy barriers, such as are associated with jogs, Peierls barriers, Frank-Reed source, nodes, forest dislocations and foreign atoms (impurities in ppm). Statistically, the configuration of the sources of drag along the lengths of the dislocations remains largely invariant in the course of their mutual interaction. The stress due to the interaction between two such dislocations will reduce the effective barrier - heights, and the activation energy for glide will progressively decrease. The velocity at which the two dislocations intersect would increase, and transitions to consecutively lower energy barriers would continue to take place until a stable " low-energy" configuration is attained, in this case the dipole "a - b".

If the available spectrum of effective barrier - heights $u_1 \leq u \leq u_2$ is divided into levels of equal widths δu, as as shown below:

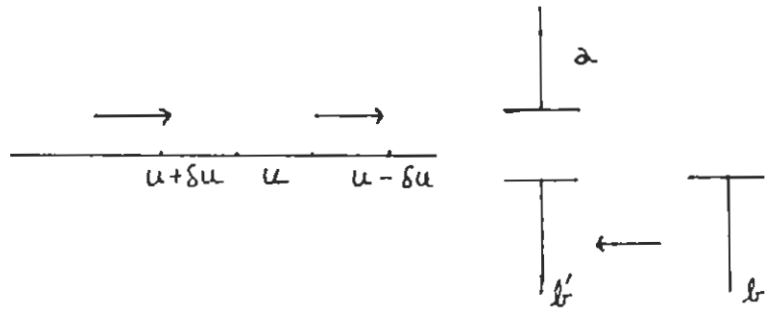

[Scheme of transition into and out of a given barrier level (left) and dipole formation (right)]

then the transitions from and to a given u - level are of the one-step type, as indicated by the arrows. Now, if the number of barriers of height u per unit volume of a crystal subjected to a constant shear stress is n(u,t). δu at time t after the onset of creep, then the influx and outflux of dislocation/barrier units from the u-level will be defined by the following relation i.e.

$$\frac{\partial n(u,t)}{\partial t} = \nu \left[n(u+\delta u,t) \exp\{-(u+\delta u)/kT\} - n(u,t) \exp(-u/kT) \right] \quad \ldots\ldots \quad (66)$$

We now assume the continum approximation for the finite difference term, one has from eq.(66).

$$\frac{\partial n}{\partial t} = (\nu\ \delta u)\ \partial \left[n \exp(-u/kT) \right] \Big/ \partial u \quad \ldots\ldots \quad (67).$$

where ν is vibrational frequency of the order of 10^{11}/sec. Introducing the transition probability on eq (67), we have

$$N(u,t) = n(u,t) \exp(-u/kT) \quad \ldots\ldots (68)$$

Suppose $\phi = \exp(u/kT)$ ... (69), one finds that

$$\frac{\partial N(\phi,t)}{\partial t} = D\partial N(\phi,t)/\partial\phi \text{ where } D = \nu\delta u/kT \quad \ldots. (70)$$

which has the general solution

$$N = Z(\phi+Dt) \quad \ldots\ldots\ldots (71)$$

If each transition of a slip unit between consecutive barriers is assumed to make the same contribution to the over all strain , then the strain rate is proportional to the integral of N (u,t) over the available u-spectrum.

Considering the specific form of N (eq.70) i.e.

$$N \propto \exp -\left[(\phi+Dt)/\phi^* \right]; \ \phi^* = \text{constant} > 0 \quad \ldots. (72)$$

so that $n(\phi,o) \propto \phi \exp(-\phi/\phi^*)$ ..... (73)

As in practice, $u >> kT$ within the u-spectrum, the n-distribution at $t = 0$ will be narrow, and one would expect the creep function with an apparent single activation energy u^*, close to u_1. Variables in eq (72) are separable. It is readily confirmed by integration, first with respect to u, and then with respect to t, that the creep strain is given by

$$\varepsilon = \varepsilon_\infty \left[1 - \exp(-t/t^*) \right], \ t^* = \phi^*/D \quad \ldots. (74)$$

where ε_∞ will depend on u_1, u_2, temperature etc but not on t.

A second solution of eq (70) obtained by Buckle and Feltham (52) with a "box-shaped" initial u-spectrum i.e. $n(u,0)$ is constant over the u-spectrum is indistinguishable from the common logarithmic relation i.e.

$$\varepsilon = s \log(1 + t/t_o) \quad \ldots\ldots (75)$$

where $t_o = \left(\frac{1}{D}\right) \exp\,(u_1/kT)$

which they use to represent their results on the creep of aluminium and copper at room temperature. As eq (70) is linear, one can, in view of eq (75), obtain an another possible solution i.e.

$$\varepsilon = s \log \left[(1+t/t_{o1}) \Big/ (1+t/t_{o2}) \right]; \; t_{o1} << t_{o2} \quad \ldots (76)$$

which requires testing on creep curves for crystals.

We can also obtain a "power-law" solution applicable to creep, from eq (75) i.e. on writing

$$\ln (1+t/t_o) = (t/t_o)^m \qquad \ldots\ldots\ldots (77)$$

one finds on computing m - values satisfying eq (77), that for

$$3 \leq t/t_o \leq 1000 \; ; \; 0.28 \leq m \leq 0.38 \qquad \ldots\ldots\ldots (78)$$

i.e. over a wide, frequently encountered, range of t/t_o, values of "logarithmic - creep is represented by the well known Andrade 1/3 - power law, with m in the range of 0.33 ± 0.05.

From the above discussions, we observe that simple stochastic model considered above accounts satisfactorily for the functional forms of creep, and hence associated stress-relaxation functions.

STRESS RELAXATION MODEL:

Evidence has accummulated in the last few years that at low temperatures, generally below about 70K, anomalies exist in the mechanical response of metals and alloys. The rate determining process involved in logarithmic creep and

stress relaxation at low temperatures, where no diffusional recovery effects occur, has not been identified with certainty. After reviewing a simple stochastic model of creep (52), we believe that previous models based on the passage of isolated dislocations over a slip plane containing a dispersion of activable obstacles are too extensively abstracted from reality to be able to entrain the low temperature mechanical anomalies. The structural effects, such as strain enhancement and stress raising effects which occur in the deformation process at low temperatures have been studied by Raza (53) which confirms to the fact that the rate determining processes in logarithmic creep and stress relaxation cannot be well explained from simple stochastic models (51,52). Our model on creep (50) is simply an extension of previous models (51,52) but accounts well the functional form of logarithmic creep at low temperatures; and deals only with single and unified kind of barrier.

We developed a simple model (54) for stress relaxation in which movement of dislocations over a volume dispersion of obstacles required dislocation/dislocation interactions. Dislocations formed during deformation interact and some destroy mutually, as discussed by Mughrabi and Essman (55), suggest that some dynamic recovery processes are occuring at low temperatures. Such a process includes intersection, thus requiring a spectrum of energy not in the minimum energy configuration (50,52) but in the extended energy configuration due to catastrophic break away of dislocations.

Now, we consider the relation for the creep rate (52), i.e.

$$\dot{\varepsilon} \propto \frac{1}{t} \ln \left(\frac{1+Dte^{-u_1/kT}}{1+Dte^{-u_2/kT}} \right) \qquad \ldots\ldots\ldots (79)$$

where $D = \nu(\delta u/kT)$ and ν is the Debye frequency of the order of 10^{11}/sec. The constant of proportionality in eq (79) will generally depend on the applied stress and on temperature, which could be evaluated by the method (51). Here, we shall restrict considerations only to the functional form of eq (79). At sufficiently low temperatures, $Dte^{-u_2/kT} >> 1$; eq (79) will reduce to

$$\dot{\varepsilon} \propto \frac{1}{t} \left(\frac{u_2-u_1}{kT} \right) \qquad \ldots\ldots (80)$$

Eq (80) shows that the strain rate for the creep is purely logarithmic. Now, if creep is observed at very low temperatures, then the most probable value of u_1 i.e., u^* in the spectrum $u_1 \leqslant u \leqslant u_2$ will be (classically) about mkT, where m = 25,(51) and we can write approximately that

$$u_1 = u^* (1-\sigma/\sigma^*), \; u_2 = u^*(1+\sigma/\sigma^*) \quad \ldots. (81)$$

where σ^* depends on internal stress. As $u^* = mkT$, we have from Eq (81).

$$u_2 - u_1 = 2mkT \frac{\sigma}{\sigma^*} \qquad \ldots. (82)$$

In substitution of eq (82) in eq (80) we obtain

$$\dot{\varepsilon} \propto \frac{1}{t} \frac{\sigma}{\sigma^*} \qquad \ldots. (83)$$

Eq (83) is the strain rate for creep. Similarly, the stress rate will, therefore, be;

$$-\dot{\sigma} \propto \frac{1}{t} \cdot \frac{\sigma}{\sigma^*} \equiv -\frac{d\sigma}{\sigma} \propto \frac{dt}{t} \cdot \frac{1}{\sigma^*} \quad \ldots\ldots (84)$$

which at integration yields

$$\sigma(0) - \sigma \propto \frac{\sigma(0)}{\sigma^*} \cdot \ln\left(\frac{t}{t_o}\right) \quad \ldots\ldots (85)$$

where t_o is the constant of integration. If $t << t_o$ then the assumption $Dte^{-u_2/kT} >> 1$ is violated and the model for the creep rate (51), i.e., $-\dot{\sigma} \propto \dot{\epsilon}$ (constant), will become valid. Since we know that for stress relaxation curves (56,57), $t >> t_o$; we therefore, meet this requirement semiempirically in eq. (85) and write

$$\frac{\sigma(0) - \sigma}{\sigma(0)} = \frac{1}{\sigma^*} \ln \frac{t}{t_o} = \frac{1}{\sigma^*} \ln \left(1 + \frac{t}{t_o}\right)$$

$$\frac{\sigma(0) - \sigma}{\sigma(0)} = K^* \ln \left(1 + \frac{t}{t_o}\right) \quad \ldots\ldots (86)$$

Also, eq (84) can be written more precisely in the form

$$-d\ln\sigma \propto \frac{1}{\sigma^*} d\ln t \equiv \frac{d\ln\sigma}{d\ln t} = -C^*,$$

$$\sigma = A^* t^{-C^*} \quad \ldots\ldots\ldots (87)$$

where A^* and C^* are constants for $t >> t_o$ critical. We conclude from eqs. (86) and (87) that the stress relaxation is "athermal" and logarithmic in character at sufficiently low temperatures, which is in accord to the experimental results on copper single crystals, obtained by Dotsenko and Landaue (58). They found the strain rate sensitivity below about 45 K temperature independent and logarithmic in character. Therefore, the relation for a single valued activation energy, as suggested by Buckle and Feltham (52) does not seem

appropriate.

SELF-CONSISTENT STRESS RELAXATION MODEL:

Anomalous work hardening behaviour (59) and its influence on the stress sensitivity of the relaxation rate in polycrystalline metals at low temperatures (60) explained much of the resolved problems (61, 62, 63, 64, 65). Recently, Hamersky and Trojanova (66) have analysed the shape of the relaxation curves under similar assumptions in the case of creep (57). Their predictions are based on qualitative interpretations of the results which are, however, not adequately defined. Observations about upward curvature in the stress sensitivity of the relaxation rate in polycrystalline nickel at 295 K and the downward curvature in polycrystalline copper and nickel below 77 K, of Raza and Butt (60) confirm the experimental results of Hamersky and Trojanova (66).

Now, we consider stochastic model of Buckle and Feltham (52), and suggest a more modified relationship for calculating the activation energy. We developed a self-consistent stress relaxation model (67) on conditions that there would correspond continuous strain hardening of the specimen during stress relaxation. The same phenomenon happens in case of constant and logarithmic creep. Hence, the strain rate sensitivity of the relaxation rate for each stress-relaxation curve during work hardening, i.e. s_{relax}, can be calculated from

$$s_{relax} = s_{creep} = \frac{d\sigma}{d\ln \dot{\varepsilon}} = \frac{kT}{V^*} \qquad \ldots\ldots (88)$$

where V^* is the activation volume.

Now, consider the specimen in the tensile machine, with C denoting the elastic cell.

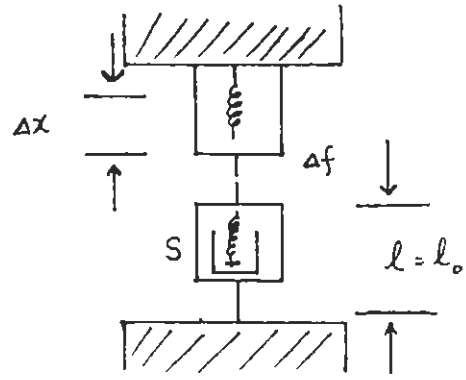

Model diagram of the Instron Machine with load cell C and specimen S

The machine is just assumed to have stopped, with the separation of the plates (shaded) fixed. Due to relaxation of the specimen (which will creep somewhat), the force will drop in the course of time, so indicating the relaxation. Now, as the separation of the plates is fixed, the strain of the specimen following stoppage of the machine (t = 0) will lead to an elongation $\Delta\ell = \ell\ \Delta\varepsilon$, where $\Delta\varepsilon = \varepsilon - \varepsilon_o$ and ℓ being the length of the specimen (we neglect changes of ℓ with time) which we regard as constant:

$$\Delta\ell = \ell\ \Delta\varepsilon \qquad \ldots\ldots\ (89)$$

Now, if M is the spring constant of the cell, then

$$\Delta f = M.\ \Delta x \qquad \ldots\ldots\ (90)$$

where Δx is the change in length of the cell due to Δf. We have

$$\Delta x = - \Delta \ell \qquad \ldots\ldots\ldots (91)$$

as the plates maintain a fixed spacing, so that

$$(\Delta \ell \equiv)\ \ell\, \Delta\varepsilon = \Delta f/M = \Delta\sigma A/M;\ \Delta\sigma = \sigma_o - \sigma \qquad \ldots\ldots (92)$$

where A is the cross-sectional area of the specimen. Thus, from eq (92).

$$-\dot{\varepsilon} = \frac{A}{\ell M}\dot{\sigma} \quad \text{or} \quad -\dot{\sigma} = \frac{\ell M}{A}\dot{\varepsilon} = E'\dot{\varepsilon} \qquad \ldots\ldots (93)$$

Eq (93) suggests that the creep rate $\dot{\varepsilon}$ is not instrument dependent and a function of the relaxation rate; it will depend on the spring constant of the cell and the specimen dimensions (ℓ/A). Thus, E' is not the same as the elastic modulus of the specimen, as would be the case if one considered that the over all deformation of the specimens were zero. However, $\dot{\varepsilon}_{pl} + \dot{\varepsilon}_{el} = 0 \Rightarrow \dot{\varepsilon}_{pl} = -\dot{\varepsilon}_{el} = -\dot{\sigma}/E$. Hence,

$$\dot{\sigma} = - E\, \dot{\varepsilon} \qquad \ldots\ldots\ldots (94)$$

In order to differentiate eq (94) from eq (93), we rewrite eq (93) as

$$\dot{\sigma} = -\alpha E\, \dot{\varepsilon} \qquad \ldots\ldots\ldots (95)$$

where $E' = \alpha E$ and $\alpha = \frac{\ell M}{EA} = \frac{M}{E} \cdot \frac{\ell}{A}$ $\qquad \ldots\ldots\ldots (96)$

thus to determine α, we need to know the beam constant M, the elastic modulus E of the specimen, and its dimensions ℓ and A. Now, considering the paper by Buckle and Feltham (52), the transient creep is expressed (by their eq (77)), as

$$\dot{\varepsilon} = s_{creep} \ln\left(1+\frac{t}{t_o}\right) \qquad \ldots\ldots\ldots (97)$$

and s_{creep} (by their eq (82')) by

$$s_{creep} = 2.3\ kT\ \sigma \Big/ (u_o - mkT)\chi_I \qquad \ldots\ (98)$$

where χ is the adiabatic coefficient of work hardening and I corresponds to linear. Taking $\dot{\varepsilon}_{pl} = \dot{\varepsilon}_{creep}$ and using eq (94), in eqs (97) and (98) we have

$$-\frac{1}{E}\cdot\frac{d\sigma}{dt} = \frac{kT\sigma\ (0)}{(t+t_o)(u_o - mkT)\chi_I} = \frac{d\sigma}{2.3\ d\ln\ (t+t_o)}$$

$$= -\sigma\ (0)\ kT\beta = -\ s_{relax} \qquad \ldots\ (99)$$

where $\beta = \dfrac{E}{(u_o - mkT)\chi}$ $\qquad \ldots\ (100)$

Considering our case for stress relaxation, i.e. eq (95), we can modify eq (100) by writing

$$\beta = \frac{\alpha E}{(u_o - mkT)\chi} \qquad \ldots\ (101)$$

For temperatures T, such that $mkT << u_o$, we have

$$\frac{2.3\ kT\sigma\ (0)\ \alpha E}{u_o \chi} = s_{relax}$$

$$\Rightarrow \quad u_o = \frac{2.3\ kT\ \sigma(0)\ \alpha E}{s_{relax}\ \chi} = \frac{2.3\ kT\ \alpha(0)}{s_{relax}}\cdot\frac{M}{\chi}\ \frac{\ell}{A} \qquad \ldots\ (102)$$

(From eq (96))

Using eq (88) in eq (102), we have

$$u_o = \frac{2.3\ kT\sigma\ (0)\ d\ln\dot{\varepsilon}}{d\sigma}\ \frac{M}{\chi}\ \frac{\ell}{A} = 2.3\ \sigma\ (0)\ V^*\ \frac{M}{\chi}\ \frac{\ell}{A}$$

$$\ldots\ (103)$$

Eq (102) is the same as usual except that it has an α in the numerator. If we assume that T is so low that $mkT << u_o$, then from eq (101) we have

$$\beta = \frac{\alpha E}{u_o \chi} = \frac{1}{u_o \chi} E \frac{M}{E} \frac{\ell}{A} = \frac{1}{u_o \chi} M \frac{\ell}{A} \quad \ldots\ldots (104)$$

Large χ will lead to small β and hence (from eq (99) and eq (103)) to low relaxation rate and for small χ, to higher relaxation rate. For "large" strains, the χ-values for truly polycrystalline (compressive) specimens will be higher than (for similar E values) for course grained tensile wire specimens as the case may be in polycrystalline copper at 15K (see Fig (3) and (4) in ref.(59); therefore, $\beta_{creep} < \beta_{ten}$ (the relaxation rate for compressive specimens is relatively less than the relaxation rate for tensile specimens). Apparently, this looks reasonable from experimental results; but this is not true; in fact, otherwise the relaxation rate mechanism would become different for tensile and compressive specimens of the same material and at the same higher strain.

What seems important is the geometrical dimension of the specimens and the spring constant (load cell) which must be taken into account for accurate calculations of the relaxation rate and hence the activation energy. This is why the activation volume for each of the stress-relaxation curves is the important parameter for more accurate calculations of activation energies. Activation volume and its dependence on adiabatic work hardening, effective stress level, and temperatures can be reasonably estimated from the analysis of stress relaxation curves in different stages of work hardening. We, therefore, conclude that the geometrical dimensions of the specimen and the spring constant itself have a great influence

on the accurate measurement of the activation energy in relaxation rate processes.

B - COMPUTER SIMULATION OF DISLOCATION MOTION :

The short range barriers are used to control the motion of dislocation or dislocations on a slip plane; these short range barriers can be overcome by thermal fluctuations. Long range barriers cannot be overcome by thermal fluctuations.

The short range barrier may be either the Peierl's stress or a solute atom or another dislocation.

Computer simulation of thermally activated dislocation motion on a slip plane is considered for the following cases:

i) A dilute random array of discrete barriers.
ii) A dilute random array of discrete barriers combined with Peierl's stress.
and iii) a group of dislocations on the same slip plane.

Fortran library of Numerical Algorithm Group (NAG) with particular reference to simulation techniques was used. Special software packages were built at ICTP. We employed these packages pertaining to simulation procedures for Pseudo-Random Generators (two dimensional array), Monte-Carlo method for quadratures and Runge Kuta method for finite dislocation advancement around pinning points, during our stay at ICTP. VAX-11/730 and CRAY - main frame computers were used.

Foreman and Makin (68) attempted to determine the stress required to move a dislocation through a two dimensional random array of point barriers at 0 K. They made two assumptions:

First, the line tension was considered to be:

$$\Gamma = \frac{1}{2\mu b}^2 \qquad \text{-----(105)}$$

where μ is shear modulus and

b is Burger's vector, and so the dislocation segments under the influence of an applied shear stress (τ) bow into arcs of circles of radius $R = \mu\, b/2\tau$. There was, however, no account taken for elastic interactions between different parts of dislocations.

Second, dislocations were assumed to break away from barriers when the angle between the arms of the dislocation reaches value θ; a parameter which characterizes the strength of the barrier. The total force exerted on the barrier by the dislocation line will be, therefore;

$$F = \mu b^2 \cos \frac{\theta}{2} \qquad \text{-----(106)}$$

where θ is shown in Fig (7).

For $\theta = 0$, the barrier has maximum strength and hence must be encircled by dislocation; and for $\theta \sim \pi$, the barrier is weak.

The method adopted by Foreman and Makin(68) was that some small value of τ was chosen and the dislocation was allowed to move forward until it made point contact with barrier or barriers. Then θ was obtained and calculations were made to check whether force on any barrier due to dislocation was greater than the maximum force of the barrier. The breaking angle θ was compared with the angle obtained

from the radius calculation. For breaking away of dislocations from barriers, dislocations move forward and the same process is created again, when further motion was not possible, the stress was increased just enough to cause breaking through and search was made for new stable configuration. After 4 to 6 stress increments - the dislocation completely traversed the slip plane without encountering a stable position as shown in Fig (8) and stress at which this occured is called flow stress or critical shear stress for the array.

However, provision was made for the dislocation to leave dislocation loops around strong groups of barriers.

Fig (9) shows variation of τ with the breaking angle θ; for the range $\theta = 0$ to π. It is observed that τ is everywhere less than τ for a square array of barriers and this difference is more clear for weak obstacles, i.e. for ($\theta \sim \pi$). Also the characteristics of the dislocation movement change with θ i.e; when θ was small, the dislocation line is very flexible due to high stress and possesses tendency to penetrate the array deeply along paths of easy movement causing encirclement of groups of obstacles. When θ was large i.e; $\theta \sim \pi$, the low stress allowed the dislocation to remain relatively straight and parallel to the bottom of the array and moves sideways by an unzipping mechanism. The same result was obtained by Kocks (69) as by Foreman and Makin (68) for single barrier using statistical theory which be defined as a perculation theory. This result was again confirmed by Hanson and Morris (70). While Scattergood and Dos (71) considered the

influence of dislocation self stresses for strong barriers i.e; they assumed interaction stresses between the arms of the dislocation as it bowed out around a barrier.

For array consisting of barrier of two different strengths, in particular two fairly weak barriers, then the stress is given approximately by R.M.S. of the stresses of the two arrays is;

$$\tau^2_{s+w} = \tau^2_{w} + \tau^2_{s} \qquad \text{----- (107)}$$

where τ_s is the stress required to move the dislocation through an array of only weak barriers. and τ_w is stress for strong barriers.

An identical result was obtained from analytical analysis by Koppenaal and Wilsdorf (72). In simulation used by Foreman and Makin (68) it was assumed without error that the drag on the dislocation is very small showing that no stress is required if a dislocation is moved between barriers. However, a finite drag is present on dislocation when barriers exist in square array. The same concept is presented by Frost and Ashby (73). A time dependent solution for the dislocation shape was obtained as a function of breaking angle θ; a method completely different than that of Foreman and Makin (68) and the angle ψ is determined as shown in Fig (7) and (10).

The shape of dislocation was obtained by a force balance over the given length of dislocation as;

$$V\beta = \tau b - \Gamma \kappa \quad \text{----- (108)}$$

where V is the velocity of dislocation,

β is the drag co-efficient,

τ is the applied stress, Γ is line tension

κ is the curvature of the dislocation. They employed no corrections for interactions between segments of the dislocation line.

Fig (11) shows the average velocity as a function of stress, and the average velocity is defined as:

$$V_{FA} = \frac{2R_o}{t_1 + t_2} \quad \text{----- (109)}$$

where t_1 is the time for the dislocation to bow out before breaking through the barriers and

t_2 is the time for travel between rows of barriers

Any stress having value below breaking stress which is defined by breaking angle ψ a dislocation does not move. Dislocations approach limiting velocity for stress above τ. Then the jumping probability was also considered by Frost and Ashby (73) by calculating the time required to jump the barrier as a function of bow out between barriers. The mean-time for jump is given by:

$$t_i = \frac{1}{\nu} \exp \frac{\Delta G(\Delta\tau)_i}{kT} \quad \text{----- (110)}$$

where ν is attempt frequency as defined by $\nu = (\nu_D b)/2R_o$ and ν_D is the Debye frequency and;

$\Delta G\ (\tau)$ is the activation free energy;

which is a function of stress.

As ψ is function of time the force acting on barrier is also function of time, so eq (110) can be written as;

$$t_i = \frac{1}{\nu} \exp \frac{\Delta G\ (\Delta\tau, t)_i}{kT} \qquad \text{----- (111)}$$

where ΔG is a function of τ and t (time). Following above considerations, Frost and Ashby (73) employ the given statistics: i.e; the probability of jumping in a time interval Δt is given:

$$\rho\ (\psi)\Delta t = \nu\Delta t \quad \exp \frac{-\Delta G(\tau, t)_i}{kT} \qquad \text{----- (112)}$$

The probability that such thermally activated jumping occurs at t in an interval Δt, is the probability that jumping has not yet occurred times the probability that it will occur in Δt.

i.e:

$$P(t)\Delta t = \left[1 - \int_o^{t-\Delta t} P(t')\, dt'\right] \rho(\psi)\Delta t \qquad \text{-----(113)}$$

This is defined as "conditional" or "prolong" probability. Then the velocity over the distance $2R_o$ will be:

$$\bar{V}_{FA}\ (t_i) = \frac{2R_o}{t_i + \left\{\left[2R_o - Y_{av}(t_i)\right] \Big/ V_{lim}\right\}} \qquad \text{----- (114)}$$

$$\text{or;} \quad \bar{V} = \int_o^{\infty} \bar{V}(t_i)\ P(t_i)\ dt_i \qquad \text{---------- (115)}$$

their computer model for dynamic bow out of dislocations

yielded ψ (t) and $\bar{V}_{FA}$ (t_1) values. These data were used to find P(t) and thus to evaluate average dislocation velocity Fig (12). It indicates that the velocity does not actually go to zero but becomes very small.

THERMALLY - ACTIVATED DISLOCATION MOTION THROUGH RANDOM ARRAYS:

Dorn and Coworkers (75) and Aresenault and Cadman (76) considered the computer simulation investigations of the thermally activated dislocation motion through a random array of barriers. The investigations of Aresenault and Cadman (76) will be reviewed and where differences and similarities of the Aresenault and Cadman and Dorn and Coworkers occur will be presented. We adopted the following procedure: A random distribution of barriers was placed on the slip plane assuming internal stress to be zero; and the minimum seperation between barriers was 1b. The force distance diagram of the barrier was a step function as shown in Fig (13). A dislocation initially enters the slip plane and moves at a drag velocity given by:

$$\bar{V}_D = \beta\tau \qquad \text{-----} \quad (116)$$

where β is the drag co-efficient and

τ is the applied stress.

since the long - range internal stress is zero so; $\tau = \tau^*$ which is the effective stress, however, when the dislocation makes contact with a barrier, then force balance is given by eq.(105) and the bow out between the internal points of contact occurs as a circular arc defined by $R = \mu b/2\tau$. Further when the dislocation is bowing out, a search is made to determine

if pinning contact is made with other barriers; if such contact is made then a new force balance has to be obtained at each point of contact; then, again the dislocation bows out between each barrier where contact is made and once more a search is made; the process continues till an equilibrium force balance is obtained which is defined in Fig (13) and the other position of force equilibrium is defined by eq.(105) In case, when a step function is used to define the force distance diagram, the positions of the force equilibrium are defined directly by the step function. This factor and force distance diagram used to reduce the computer time involved in making the calculation, but still immense amount of computer time was required to obtain a force balance. We know that if applied force F_A is greater than the strength of the barrier F_{max}, the dislocation is allowed to move over the barrier, and whole process is repeated. The strength of the barrier is only defined in the Y-direction. This is necessary to obtain the Y-component of the total force as given by eq. (105) but this is not necessary for point barriers. In case when a force balance is obtained and there are no points of contact where $F_A > F_{Max}$ then the time required to overcome each barrier where contact is made, is obtained by eq(110) while activation is given as:

$$\Delta G\ (\tau)_i = \int_{Y_1}^{Y_2} F(Y)dy - F_{Y_1}(Y_2 - Y_1) \quad ----(117)$$

where the limits of integration are obtained from force balance and F(y) by delta function. We now make the following

analysis: If the dislocation is in contact with N_i barriers, then the question arises which one or ones does the dislocation decide to jump. Six different selection methods have been investigated and some of these are described by Aresenault and Cadman (77). Dorn and Coworkers(75) used an accumulated time method. However; Morris and Kalhn (78) obtained the mean time for jumping N_i barriers in contact with dislocation by using exponential probability statistics. The Monte Carlo method was used to select barriers to be jumped by dislocation. The same technique was used by Wynblatt (79) to select the barrier that would be jumped by the dislocation. Areseneult and Cadman (80) believe the binomial distribution method is the most realistic.

CONFIGURATION OF THE MOVING DISLOCATION:

There are two possible means by which a dislocation can traverse the slip plane depending on the concentration of barriers, the strength of the barriers, τ and T. If τ is large or the temperature is high, the dislocation moves at the drag velocity and traverse the slip plane as a straight line. If the stress is reduced or temperature is lowered so that the time required to overcome some barriers is not zero, then the dislocation line does not remain straight, even though the dislocation motion is still at drag velocity. The nature of dislocation motion is not by an unzipping phenomenon. Fig (14) is a plot of successive positions of a dislocation as it moves through random array of low strength barriers $\theta=160^0$. The Y-axis gives actual bulge which occurs

when the dislocation moves. Similarly Fig (15) gives successive positions of the dislocation when $\theta=80^{0}$. In general the dislocation moves by forming small bulge i.e; five jumps barriers in the X - direction before moving forward in Y-direction, a bulge begins to form after five - jumps along X-direction. The dislocation bulges out a number of rows (where a row is defined as Y_L/N_Y, where Y_L is the length of slip plane and N_Y is the average number of barriers in Y-direction). The magnitude of the bulge out is defined as the number of rows between the minimum and maximum advance of the dislocation. Further the dislocation begins to move laterally after and during bulge out stage which is called "unzipping". Due to this effect the portions of the dislocation which are moving more or less parallel to the X-axis advance slowly in the Y-direction. Here one of the most important parameter is the effective force on the dislocation; which is the ratio of the applied force to the strength of the barrier. If this ratio is unity, the magnitude of the bulge out is large. The parameters affecting dislocations are discussed by Cadman and Aresenault (81). The observation that the "unzipping" tendency increases as the strength of the barrier increases contradicts the observations of Foreman and Makin (68).

STEADY STATE AND SLIP PLANE SHAPE:

This is well established that the boundary conditions and parameters that result in a steady state condition are the critical factors in determining τ vs T relation and the activation parameters vs τ and T relation. We define steady

state condition as follows: The steady state exists for a given T, τ and concentration of barriers if the average velocity ($\bar{V}$) does not change with an increase in the size of the array. Fig (16) is a plot of $\bar{V}$ as a function of the size of the array and it is obvious that $\bar{V}$ increases as the size increases. As a further check on the size, we determined ΔH as a function of size as shown in Fig (17). Therefore we define steady state by τ, T and concentration when the width of the slip plane is greater than 5.12 μ.

The τ required for dislocation motion through the array is at 0 K and obtained by considering the method of Foreman and Makin(68). If Y_L increases then the required stress increases to the true value; but if width X_L increases then the stress decreases. For thermally activated motion case the critical dimension is width. Considering here two sizes i.e; 1.28μ and 5.12μ for a given defect concentration. It is observed that for the smaller size case, if a square slip plane is used the number of barriers is $\sim$1089 if 'N' different arrays are generated then the average velocity for each array will be different, but for 3.84μ or 7.6μ in length the average velocity is almost constant i.e; $\pm$ 20% of that obtained by the average of the six arrays. For large size with the length one - half the width, the average velocity is the same as that when $X_L = Y_L$. The two worker Klahn etal(75) and Morris etal (78) employed a square array size of 999 barriers. This effect of small array size can be explained by taking two different size slip planes and using binomial selection

method. In the first case the slip plane is 0.794μ square and contains 1089 barriers; the $\bar{V}$ from six different arrays varied by ∿3 order of magnitude, but if area covered by the dislocation as a function of time is taken, then there is no practical difference as can be seen in Fig (18 a and b), this relation between distance moved and time is linear if temperature is increased and so decreasing the stress, similar relation is obtained if large size slip plane is taken keeping all other parameter same as in Fig (19). Now Hanson etal (82) have shown that at 0K, τ decreases as the array size increases.

Further study has revealed that the major contribution to the total time required by the dislocation to cross to slip plane was controlled by few jumps, four or five "hardspots". We consider hardspots as Five barriers in a rectangular area of 100b in the X-direction and 20b in Y-direction for 144 ppm concentration. After defining hardspots, we made a search of these spots on the slip plane. The dislocation was placed at a variable distance behind a hardspot and allowed to move. The dislocation was removed from the slip plane when it had jumped the hardspot and then placed behind the next hardspot. The time required for such a process cannot be found, so these negative results show that there is difference between dynamic and static hardspots. Therefore, the circle rolling technique of Foreman and Makin (68), which was used by Hanson and Morris etal (70) for determining hardspots would not be applicable for thermally activated dislocation motion. However Hanson

and Morris (82) have recently used a different technique.

In general, to have steady state conditions as the stress increases either due to increasing concentration of barriers, decrease in temperature, or an increase in strength of barriers, the size of the array necessary to produce steady state condition has to increase.

Now, as steady state condition has been determined so the activation energy and the activation area can be obtained as a function of τ and T, and τ vs T. The computer simulation results of the above relationship as shown in Fig (20) are in agreement with those predicted by Friedel (83).

Aresenault and Cadman (84) investigated the effect of barriers of two different strengths on the thermally activated motion of a dislocation through a random array of these barriers.

Therefore, we conclude that there is synergistic or coupling effect in the values of activation energies and volumes for strong and weak barriers. Moreover the activation energy obtained is not a mean value of the activation energy associated with the strong and weak barriers but is larger than that associated with the strong barrier. The stress required to maintain a given average velocity shows that is a coupling effect between strong and weak barriers as shown in Fig (21).

MULTIPLE DISLOCATION MOTION:

UNIFORM FRICTION

A computer model was developed by Rosenfield and

Hahn (85) for solving a set of differential equations for the positions as a function of time of straight coplanar dislocations emitted from a single source. The velocity of a dislocation is given by:

$$V_i = C \exp (B \tau_{eff}) \qquad \text{----- (118)}$$

where C and B are constants,

i is the index number of dislocations and τ_{eff} is the effective stress on the dislocation. This velocity stress relation is used for viscous drag situation or frictional drag situation.

Further the effective stress itself is given by:

$$\tau_{eff} = \tau_a + \tau_{di} \qquad \text{----- (119)}$$

where τ_a is applied stress and

τ_{di} is the stress on the glide dislocation due to other dislocations in the array.

This is called linear dislocation array, which was ascribed by Rosenfield and Hahn (85) as low speed screw dislocations, so that

$$\tau_{di} = \frac{\mu b}{2\pi} \sum_{\substack{i=0 \\ i \neq j}}^{N} \frac{1}{Y_i - Y_j} \qquad \text{----- (120)}$$

where Y_i and Y_j are the positions of the N-dislocations in the array. They performed calculations for different values of parameters; the results of which are shown in Fig (22). The dislocation arrangement is that of an inverse pile-up. Rosenfield and Hahn (85) relationship indicates that

dislocations after covering a short distance reach a steady state velocity which is considerably higher than that of a single dislocation. This is a surprising aspect because difference in velocity is two orders of magnitude for dilute alloys.

DISCRETE BARRIERS:

A computer simulation model was developed by Aresenault Shrovaneck and Cadman ([86]) for the motion of a group of dislocations through a random array of barriers which were or could be jumped by thermal fluctuations. The motion of multiple co-planar or parallel dislocation through a random one-dimensional array of short range barriers was examined for three different types of short range barriers. One of the barriers was chosen to represent the dislocation etch pit data obtained from Fe-Si (Stein and Low ([87])). From this data it is possible to obtain a plot of ΔH vs τ_a and also a value of τ_i.

A relation for ΔH vs τ_{eff} plot is as follows:

$$\Delta H = \Delta H_o \left[1 - (\tau/\tau_o)^{\frac{1}{2}}\right]^2 \qquad \text{----- (121)}$$

where; $\Delta H = 1.14 eV$

and $\tau_o^* = 39 Kg/mm^2$

Further it is assumed that:

$$\tau_i = 11 Kg/mm^2$$

and that τ_{di} is zero, and change in entropy (ΔS) is zero and

$$\tau_{eff} = \tau_a - \tau_i + \tau_{di} \qquad \text{----- (122)}$$

The density was so adjusted that; τ_a = 12Kg/mm^2 for velocity 10^{-8} m/sec which satisfies experimental value at that stress. Once, density for short-range barrier was determined, it was fixed and the velocity at various other stresses was obtained. The motion of a group of dislocation was then considered with this same short - range barrier density. The long - short dashed line in Fig (23) is the steady state velocity of the first of 11 dislocations generated, the velocity is nearly 1.65 times faster than that of single dislocation traversing a short - range barrier array at 300 K and 2.80 times faster at 77 K. This has been observed that velocity of any dislocation in the group approaches an average or steady state velocity after travelling two or three times the insert distances. The insert distance is the distance a dislocation that has travelled from the source before the next dislocation comes into existence at the source. Fig (24) is a plot of instantaneous velocity vs distance of the first dislocation generated; here instantaneous velocity is the distance between 10 short - range barriers divided by the time required to traverse them. Also, the maximum in the value of intantaneous velocity occurs when first dislocation has covered a distance of 10b which means that second dislocation comes into existance at the source, but no such effect is developed when third dislocation is generated at the source. Then second barrier was taken to represent the dislocation etch pit results given by Guberman (88) from Cu.

UNIFORM FRICTION VS DISCRETE RANDOM BARRIERS:

For basic understanding of differences in the data of Rosenfield and Hahn and the data of Aresenault etal (85) the differential equations defined by Rosenfield and Hahn (85) were numerically solved by Runga Kutta method. In the specific case of Cu at 77 K, it was found that the differences in the steady state velocity between the first dislocation of a multiple group and a single dislocation were less than a factor of two and nearly independent of stress; further these results obtained from the discrete barrier and the frictional resistance simulation were almost identical. A comparison of several other cases were examined and a general result is shown in Fig (25a and b). The differences in velocity between the first dislocation generated by a continuously operating source, when the source has generated 7-10 dislocations, and a single dislocation are always less than 3.

DISLOCATION REMOVAL OF BARRIERS:

Arsenault (88) investigated dynamic pile up formation for the situation where the moving dislocations had a finite probability of removing the barriers i.e; "channel" in neutron-irradiated and deformed metals. The results of this investigation show that it is possible to have slip lines form rapidly with the process still being thermally activated. A limit is imposed i.e; the rate of removal of the barriers by the moving dislocation must be small less than 10%. It is to ensure that the same possibility such as when the pile-up forms remains for the entire stress and temperature range.

If, however, the rate of removal is large, then there is possibility of discontinuties in the activation energy effective stress relation. As such a lower limit is also present at about 2-3%. Due to the removal of barriers, a dynamic dislocation pile-up forms; and if the rate of removal is small the pile-up will form after a finite number of dislocations have exited the sample. But, we found that once a dynamic pile-up forms; the further deformation on that slip plane is controlled by the rate of motion of the pile-up which is nearly the velocity of sound as shown in Fig (26).

Further, the deformation being controlled by the formation of dynamic dislocation pile-ups is that the pre-exponential terms should be large, which is in agreement with the experimental results.

CHAPTER 3.

CONCLUSIONS

- SUGGESTIONS FOR FUTURE WORK

CONCLUSIONS:

We infer from our studies the following conclusions.

- The movement of dislocations over a volume dispersion of obstacles requires dislocations/dislocation interactions at very low stress, either in single crystals or in polycrystals with coarse substructures. Therefore, the relation for single valued activation energy as suggested by Buckle and Feltham (52) does not seem appropriate because for dislocation/dislocations interactions, we need a multibarrier stochastic model for creep.

- The relation for the creep rate (51) is modified for low temperatures which suggest that the behaviour of stress relaxation rate is logarithmic in character.

- Structural effects such as strain enhancement and stress raising in the pre-yield band formation and dynamic recovery occuring at low temperatures (53) suggest that simulation of dislocation structures with reference to experimental data should be studied to develop multibarrier stochastic models.

- We believe that previous models (51,52) based on the passage of isolated dislocation over a slip plane containing a dispersion of activable obstacles were not sufficient to explain the low temperature mechanical anomalies. However, such models are indeed helpful in simulation studies which we performed using certain characteristics and parameters.

- A self-consistent stress relaxation model is developed (67) on conditions that continuous strain hardening of the specimen is produced during stress relaxation. The same

phenomenon is observed in logarithmic creep.

- Activation volume and its dependence on adiabatic work hardening, effective stress level and temperatures can be reasonably estimated from stress relaxation curves in different stages of work hardening. The same observations were recorded by Hamersky and Trojanov (66) and S.M. Raza (61,62,63,64,65).

- Self-consistent stress relaxation model which we developed (67) emphasises on geometrical dimensions of the specimen and the spring constant itself to account for the influence on the accurate measurement of activation energy in relaxation rate processes.

- Mechanical twinning is a characteristic of low temperature deformation and occurs by the movement of partial dislocations. At very low strains, cross slip is partially expected due to widening of stacking fault ribbon.

- Cross-slip is inhibited at larger strains due to strain enhancement effect. We believe that the twin surfaces are formed due to strain enhancement and stress-raising effects.

- A single barrier stochastic model of low temperature creep is developed (50) in which we have introduced dynamic recovery processes due to localised relaxation of dislocation structures in the low temperature plastic deformation of metals which justifies the dislocation structures and interaction processes.

- The angle ψ is determined from a time dependent solution for dislocation shape as a function of breaking angle θ as shown in Figs.(7) and (10). This technique is totally different than that of Foreman and Meckin (68). The shape of the

dislocation is obtained by force balance equation over the given length of the dislocation using $v\beta = \tau b - \Gamma k$ (89).

- Using computer model (73) for dynamic bow out of dislocations we calculated average dislocation velocity as shown in Fig.(12) which indicated that the velocity would never become zero (73).
- The search for pinning contact was made with other barriers thereby describing a new force balance if such contact exists. The dislocation bows out between each barrier where contact is made requiring a new search until the equilibrium force balance is obtained as shown in Fig.(13).
- Dislocations move by forming bulge i.e; five jumps barriers in the x-direction before moving forward in the y-direction, a bulge begins to form after five jumps along the x-direction.
- Our observation that "unzipping" tendency increases as the strength of the barrier increases contradicts Foreman and Makin (68).
- We define steady state by τ, T and concentration when the width of the slip plane is greater than 5.12 μ. Fig.(16) and (17) explain the increase of average velocity of dislocations with increase in the size of the array.
- We ascribe the critical dimension as width for thermally activated dislocation motion.
- In case of small size the average velocity for each array will be different except for certain caseswhere it is constant, but for large size with the length one-half the width, the average velocity is the same as when $X_L = Y_L$.

- The total time required by the dislocation to cross-slip plane was controlled by few jumps i.e; four or five hard-spots, however, there is difference between dynamic and static hardspots.

- The computer simulation results of τ and T as shown in Fig. (20) are similar to those predicted by Friedel (83).

- The stress required to maintain a given average velocity would need coupling effect between strong and weak barriers as shown in Fig.(21).

- Dislocations after covering a short distance reach a steady state velocity which is considerably higher than that of a single dislocation (90).

- Dislocation jump approaches an average or steady state velocity after travelling two or three times the insert distances.

- Results obtained from the discrete barrier and the frictional resistance simulation are indentical. Comparison of several cases were examined and shown in Fig.(25).

- Once a dynamic pileup forms, deformation on slip plane is controlled by the rate of motion of the pile-up which is nearly the velocity of sound as shown in Fig.(26). The deformation is also controlled by the formation of dynamic dislocation pile-ups. The pre-exponential terms in dynamic dislocation pileups is in agreement with the experimental results.

SUGGESTIONS FOR FUTURE WORK:

- Development of a Multibarrier Stochastic model.
- Simulation Studies with reference to single barrier stochastic model.
- Simulation studies with reference to multibarrier stochastic model.
- Interaction between individual slip units during strain hardening may require computer simulation.
- Rate of deformation in metals which is a manifestation of motion of dislocations through a crystal with high Peierls barrier especially in BCC crystals will require further studies both experimentally and theoretically on the basis of which suitable models mainly the stochastic Peierls barrier model will be developed and can be further modified using simulation studies.
- Simulation of experimental results on transmission electron microscope (TEM), high voltage electron microscope (HVEM), scanning electron microscope (SEM) and on scanning tunnelling microscope (STM) for defects and defect like structures in different metals especially at low temperatures would yield better results for development of realistic mathematical models.

FIGURE CAPTIONS

Fig. 1. Potential energy of a dislocation in the plane periodical Peierls relief and in the external stress field. u is the coordinate in the direction normal to the Peierls valleys, a is the distance between two neighbouring valleys, u_o is a kink coordinate.

Fig. 2. Two neighbouring minima (valleys) in the Peierls relief.

Fig. 3. Double kink in a dislocation: l is the double-kink length, l_o the signle-kink width 14

Fig. 4. Motion of a dislocation segment AB in the potential field of a defect 0: d is the size of the defect and of the central dislocation segment; L_1 and L_2 the left and right segment lengths; ϕ_1 and ϕ_2 the instantaneous values of the angles of attack for the left and right segments; y the coordinate of the central dislocation element 16

Fig. 5. Migration of a dislocation segment over one barrier to a new one. The second position is indicated by the broken curve.

Fig. 6. Possible transitions to and from barriers of height u.

Fig. 7. A schematic of a dislocation in contact with several barriers.

Fig. 8. Typical variation of stress with maximum penetration distance of a dislocation into a random array of width 100 L (L is the average spacing between barriers) (10^0 breaking angle); broken line is for array of 10,000 used in computations. A well-defined "yield point" is characteristic of all arrays and barrier strengths, and occurs well within the limit set by a square-shaped array.

Fig. 9. Variation of the critical shear stress τ with breaking angle θ for a random array of 10,000 barriers with 1% stress increment (solid circles), and for an array of 1,000 barriers with 2% increment (open circles). Error limits show the range of values from a series of different arrays of 1,600 barriers. The square lattice stress τ_s, Friedel stress τ_f, and empirical result τ_e.

Fig.10. Diagram illustrating the bowing of a dislocation between barriers P-P, the bow out angle ψ and the way in which the velocity $v = 2R_2/(t_1 + t_2)$ was calculated.

Fig.11. Dislocation velocity at 0 K as a function of stress for various strength barriers.

Fig.12. Thermally activated dislocation velocity v plotted against stress in units of τ_{crit}. The quantity ΔG describes the strength of the obstacle. A dislocation can move rapidly through a field of weak obstacles $\Delta G/RT = 50$ at stress levels below τ_{crit}, but strong obstacles ($\Delta G/kT = 500$) can only be cut at stress at or above τ_{crit}.

Fig. 13. Force distance diagram.

Fig. 14. The successive positions and configurations of the dislocation as it moves across the slip plane. The different types of lines represent the different locations of the dislocation .

Fig. 15. The successive positions and configurations of the dislocation as it moves across the slip plane. The different types of lines represent the different locations of the dislocation.

Fig. 16. The average velocity vs the width of the slip plane.

Fig. 17. The activation energy vs the width of the slip plane.

Fig. 18. (a) The distance traversed by a dislocation as a function of time.

(b) The area swept out by the dislocation as a function of time.

Fig. 19. The distance traversed by the dislocation as a function of time.

Fig. 20. The stress required for a given dislocation velocity (10^{-7}m/sec) as a function of temperature.

Fig. 21. The stress as a function of temperature at a given average dislocation velocity, where θ is a measure of the strength of the barriers.

Fig. 22. Movement of some individual dislocations emitted by a source. A total of 20 dislocations was generated during the calculation (Ref. 84).

Fig. 23. The steady velocity vs applied stress.

Fig. 24. The instantaneous velocity of the first dislocation as a function of distance from the source.

Fig. 25. (a) Dislocation configurations for various value of stress exponent.

(b) Dislocation configurations for various value of stress exponent.

Fig. 26. The instantaneous velocity of the first 8 dislocations as a function of distance from the source.

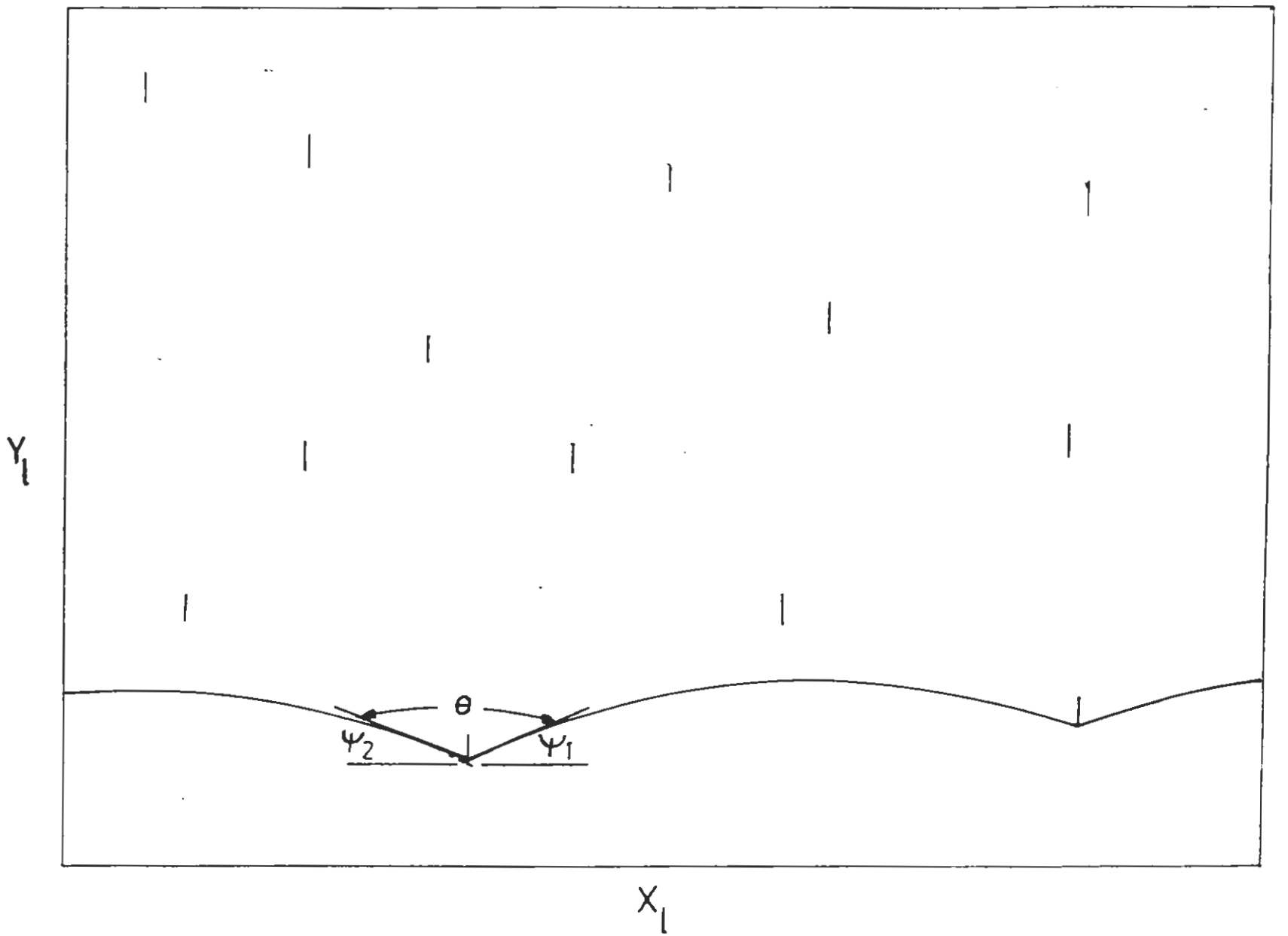

Fig. 7. A schematic of a dislocation in contact with several barriers.

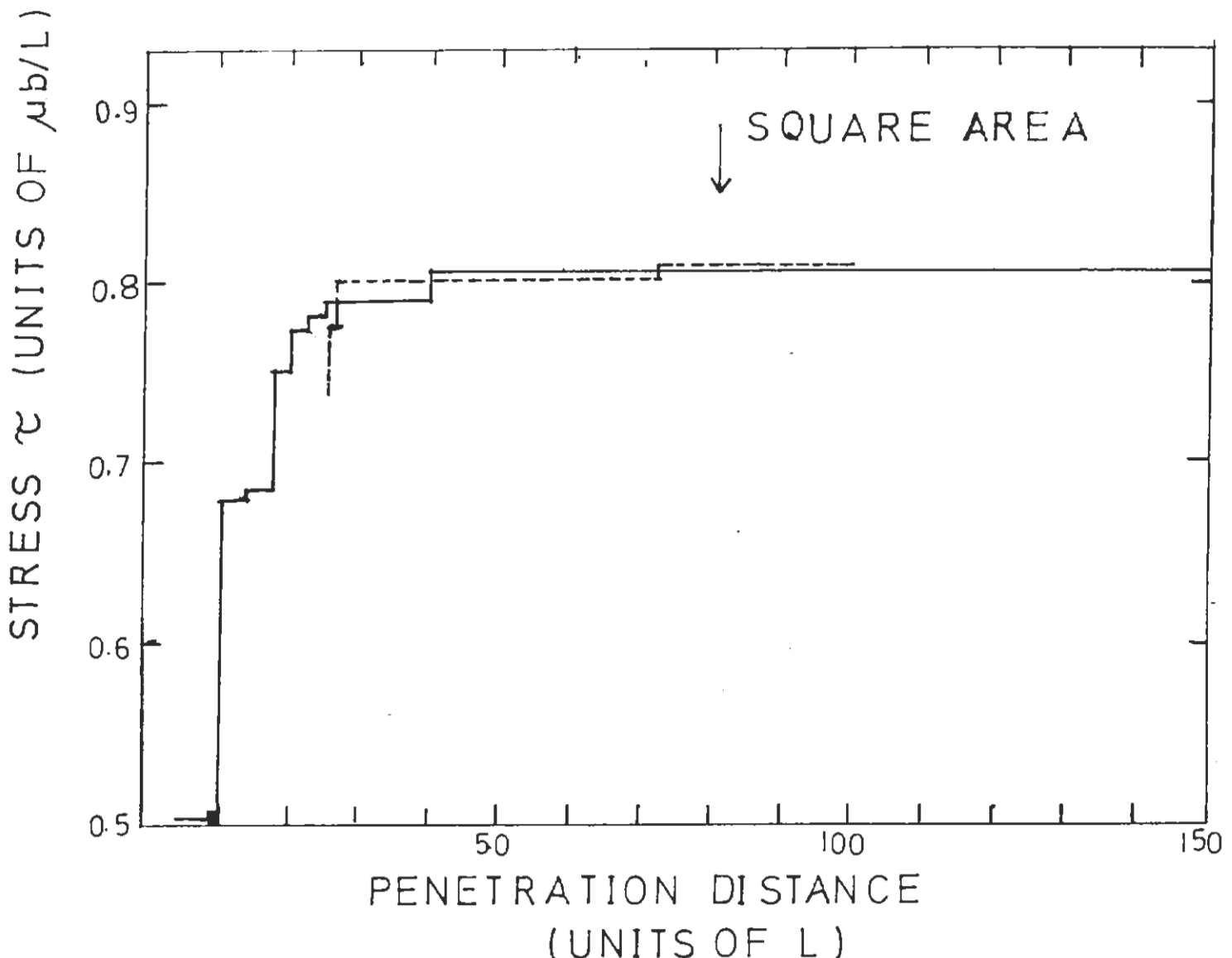

Fig. 8. Typical variation of stress with maximum penetration distance of a dislocation into a random array of width 100 L (L is the average spacing between barriers) (10^0 breaking angle); broken line is for array of 10,000 used in computations. A well-defined "yield point" is characteristic of all arryas and barrier strengths, and occurs well within the limit set by a square-shaped array.

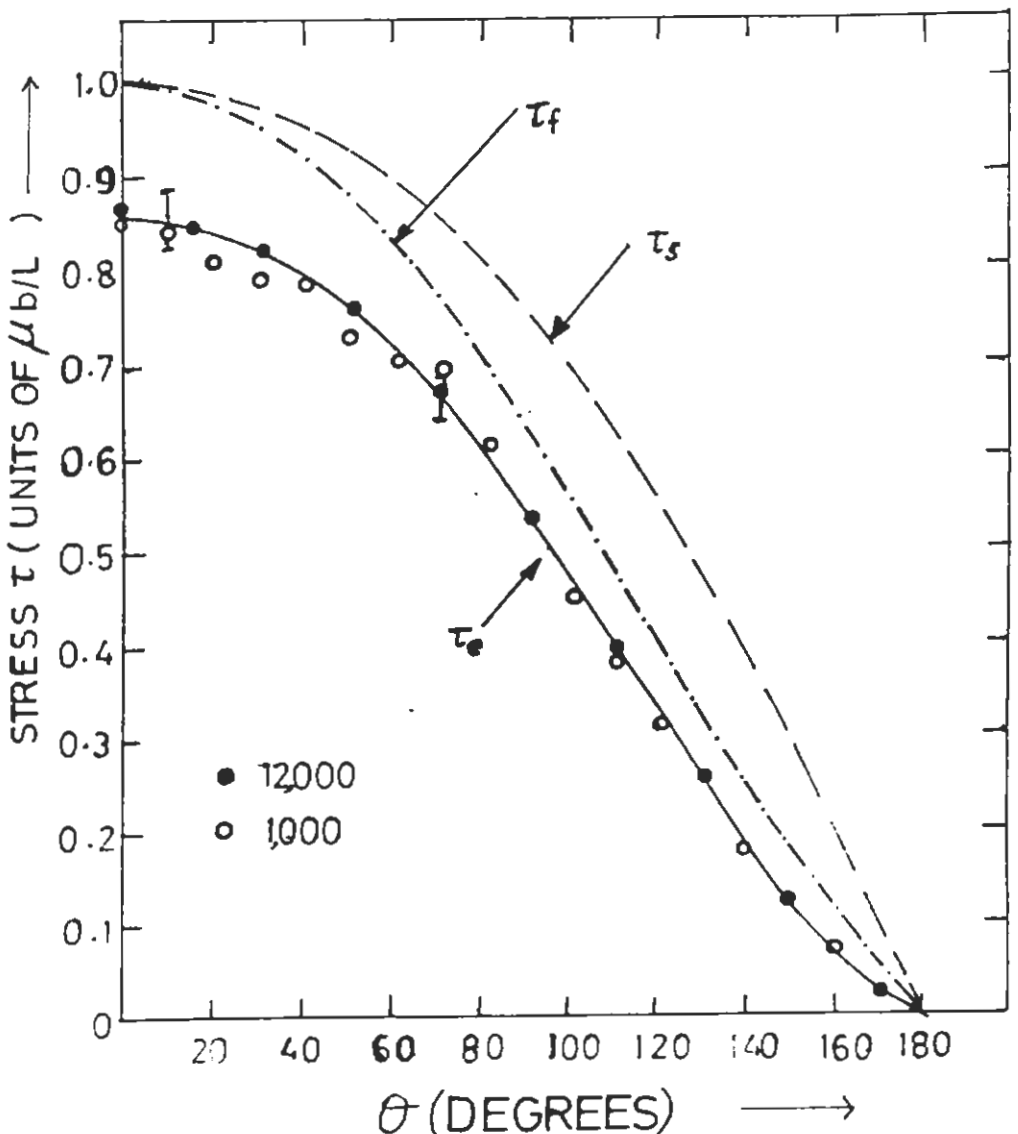

Fig. 9. Variation of the critical shear stress τ with breaking angle θ for a random array of 10,000 barriers with 1% stress increment (solid circles), and for an array of 1,000 barriers with 2% increment (open circles). Error limits show the range of value from a series of different arrays of 1,600 barriers. The square lattice stress τ_s, Friedel stress τ_f, and empirical result τ_e.

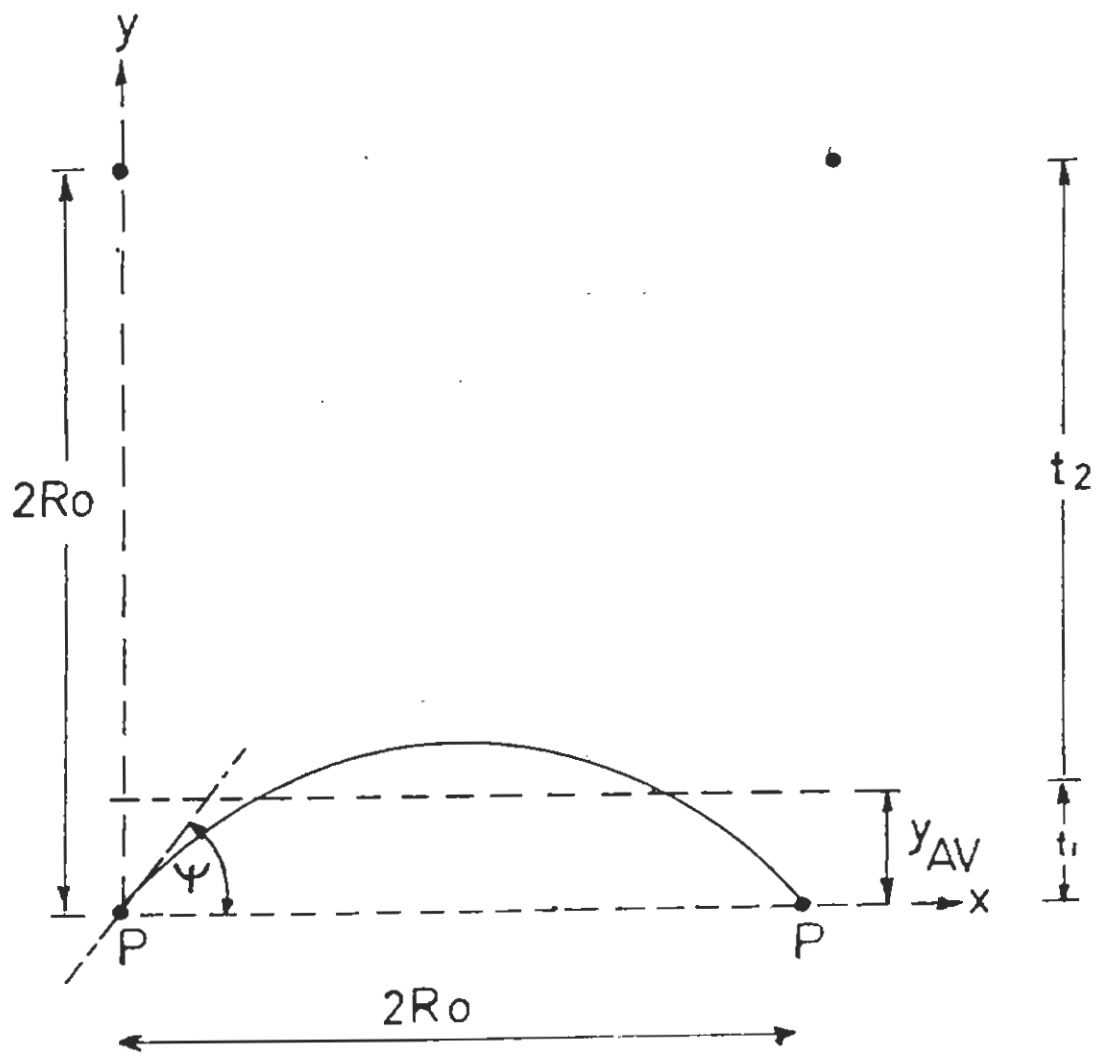

Fig.10. Diagram illustrating the bowing of a dislocation between barriers P - P, the bow out angle ψ, and the way in which the velocity $\bar{v} = 2R_c/(t_1 + t_2)$ was calculated.

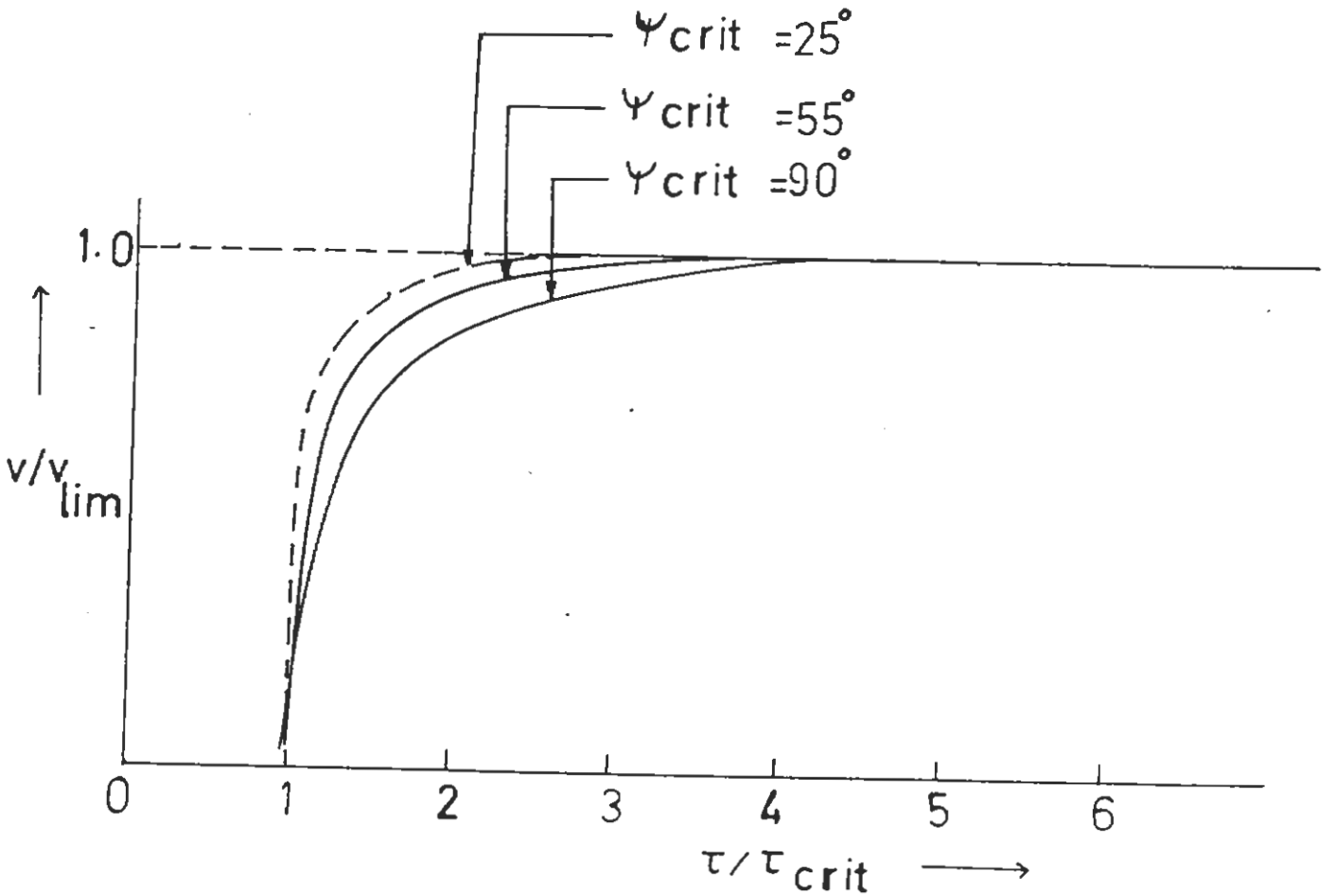

Fig. 11. Dislocation velocity at 0 K as a function stress for various strength barriers.

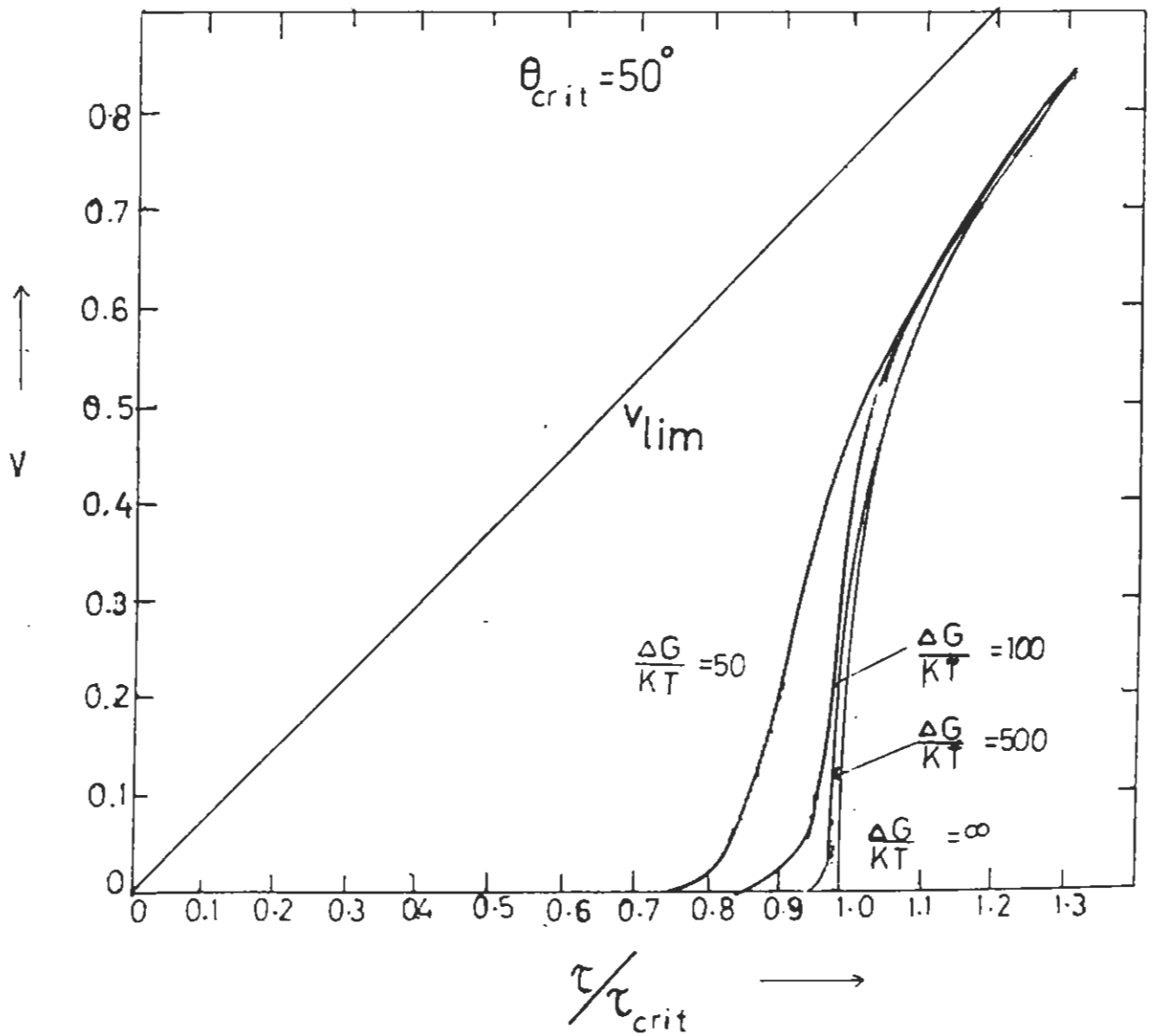

Fig. 12. Thermally activated dislocation velocity v plotted against stress in units of τ_{crit}. The quantity ΔG describes the strength of the obstacle. A dislocation can move rapidly through a field of weak obstacles $\Delta G/RT=50$ at stress levels below τ_{crit}, but strong obstacles ($\Delta G/kT = 500$) can only be cut at stresses at or above τ_{crit}.

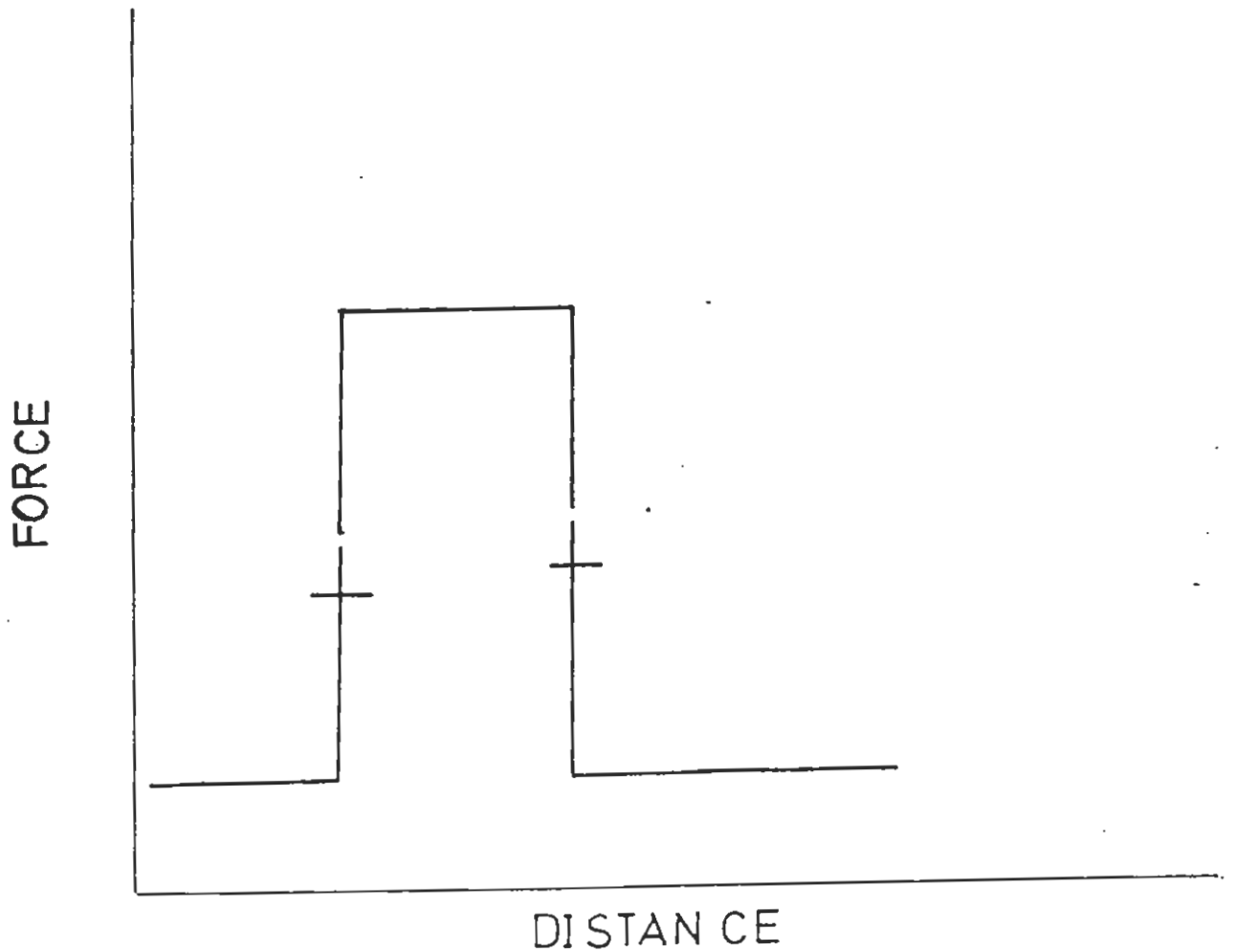

Fig.13. Force distance diagram.

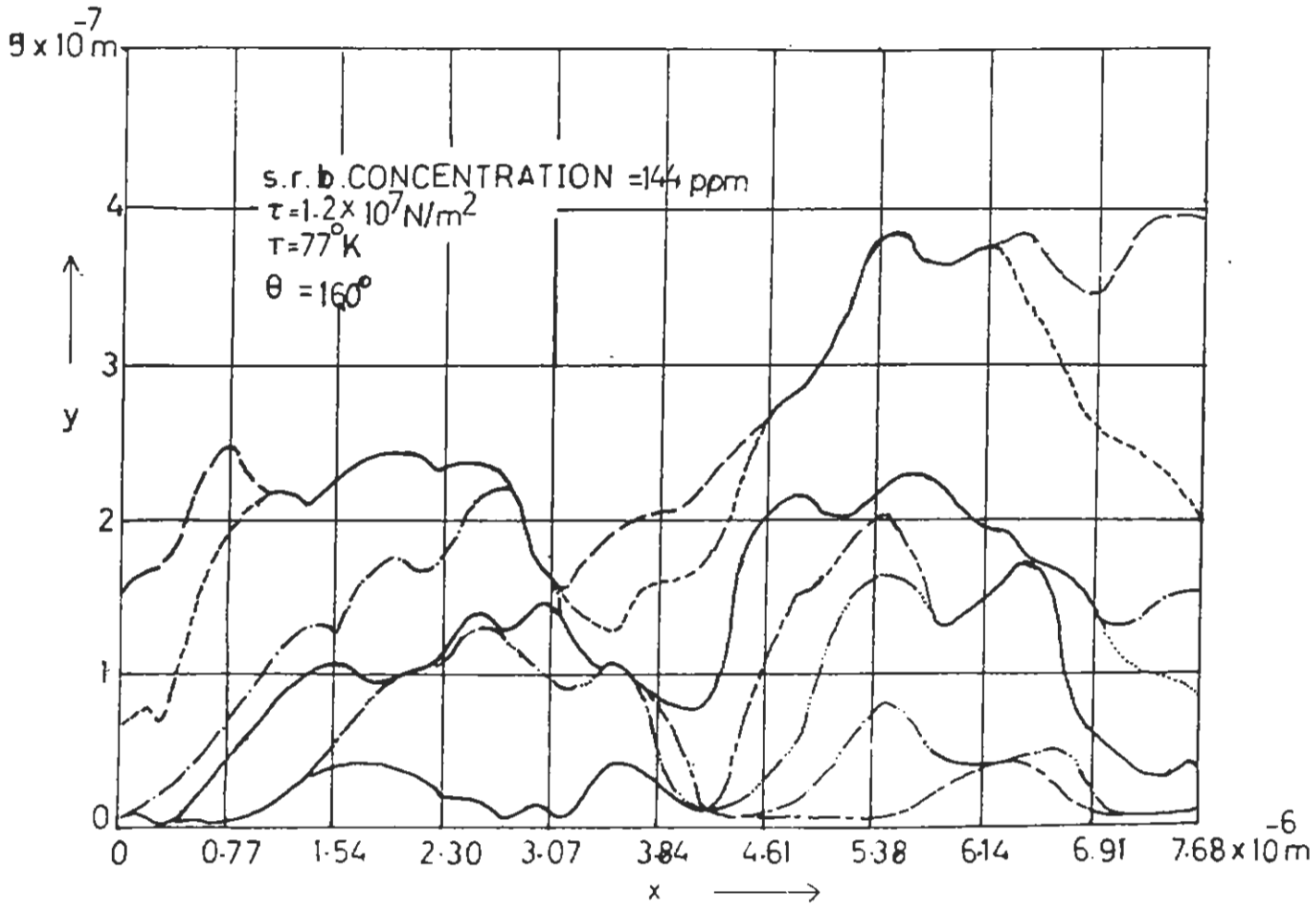

Fig. 14. The successive positions and configurations of the dislocation as it moves across the slip plane. The different types of lines represent the different locations of the dislocation.

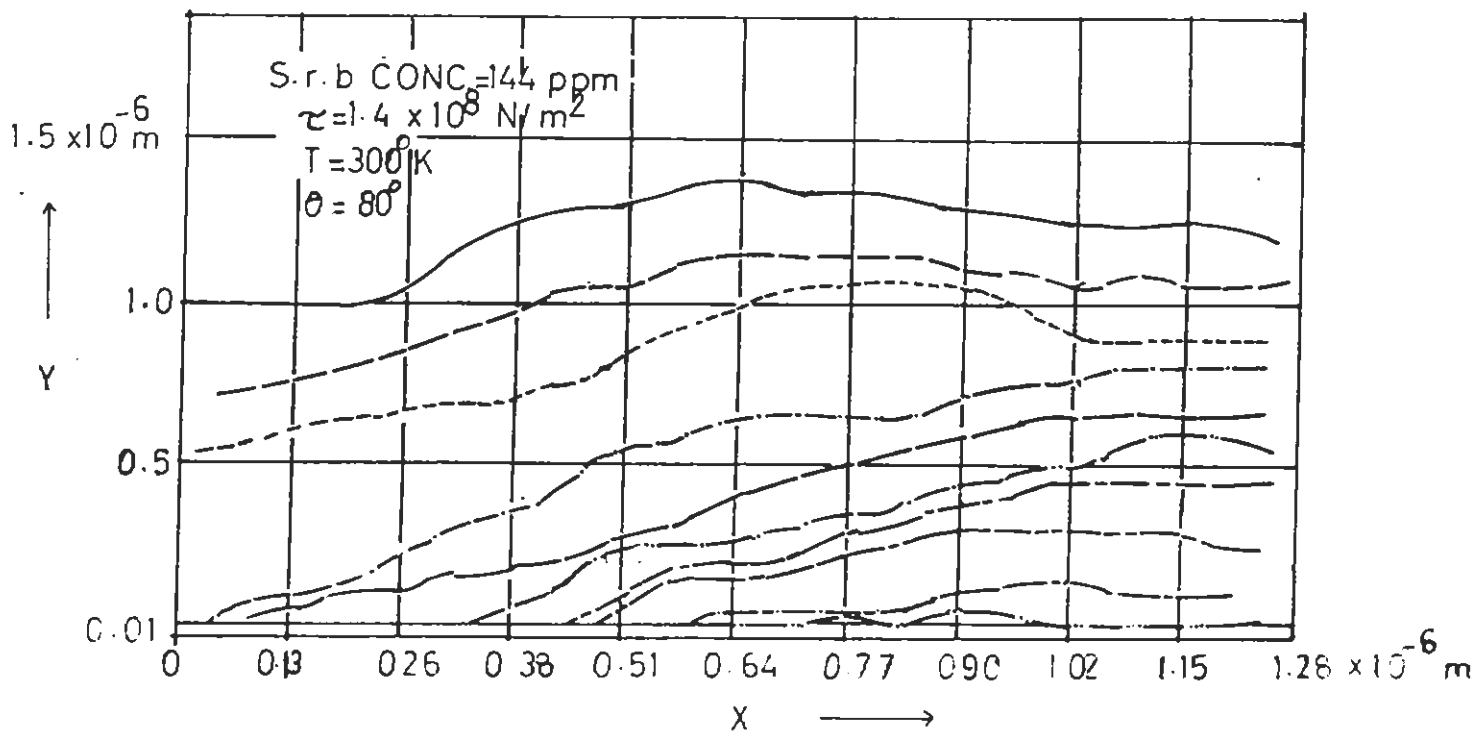

Fig.15. The successive positions and cnfigurations of the dislocation as it moves across the slip plane. The different types of lines represent the different locations of the dislocation.

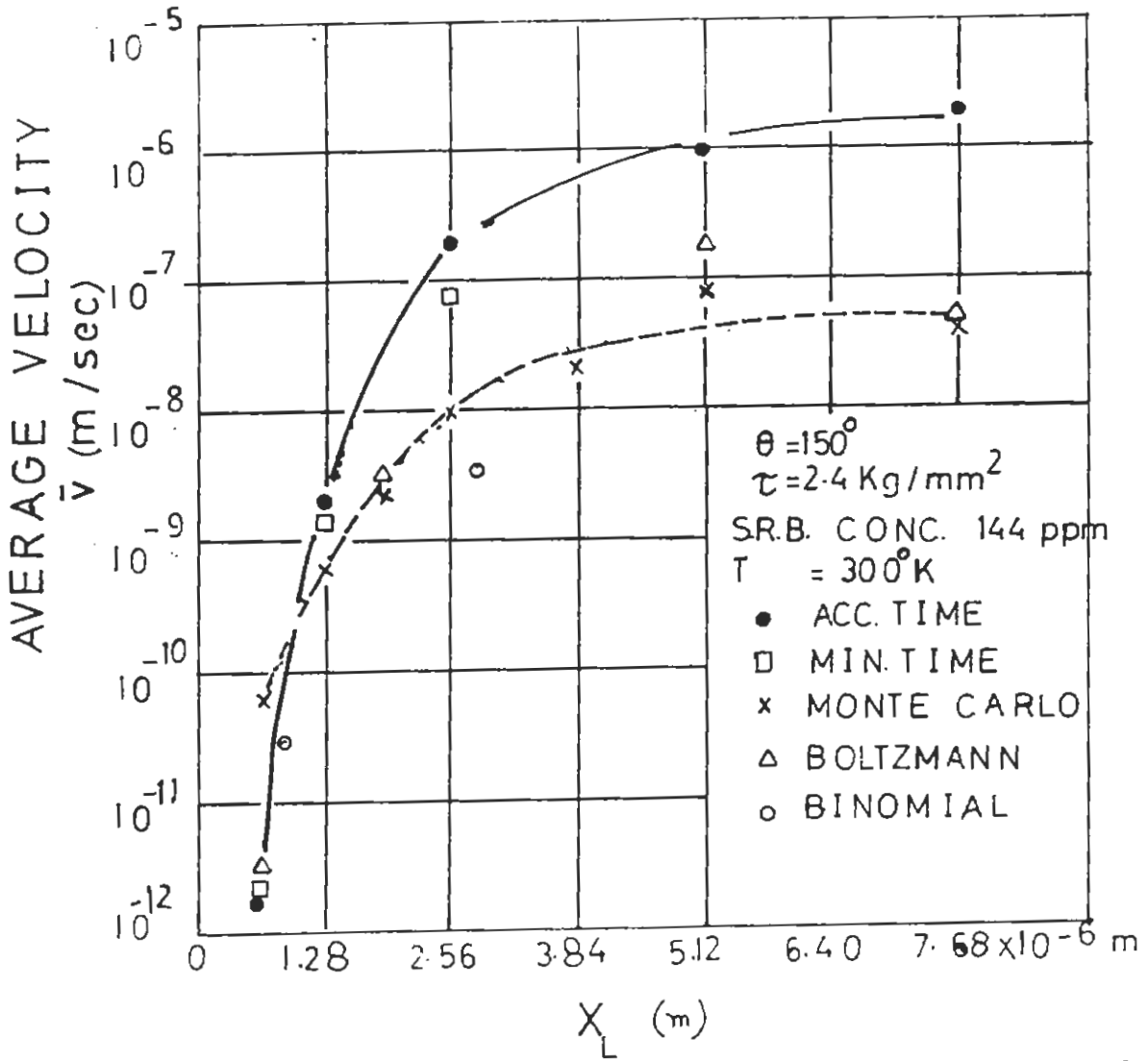

Fig. 16. The average velocity vs the width of the slip plane.

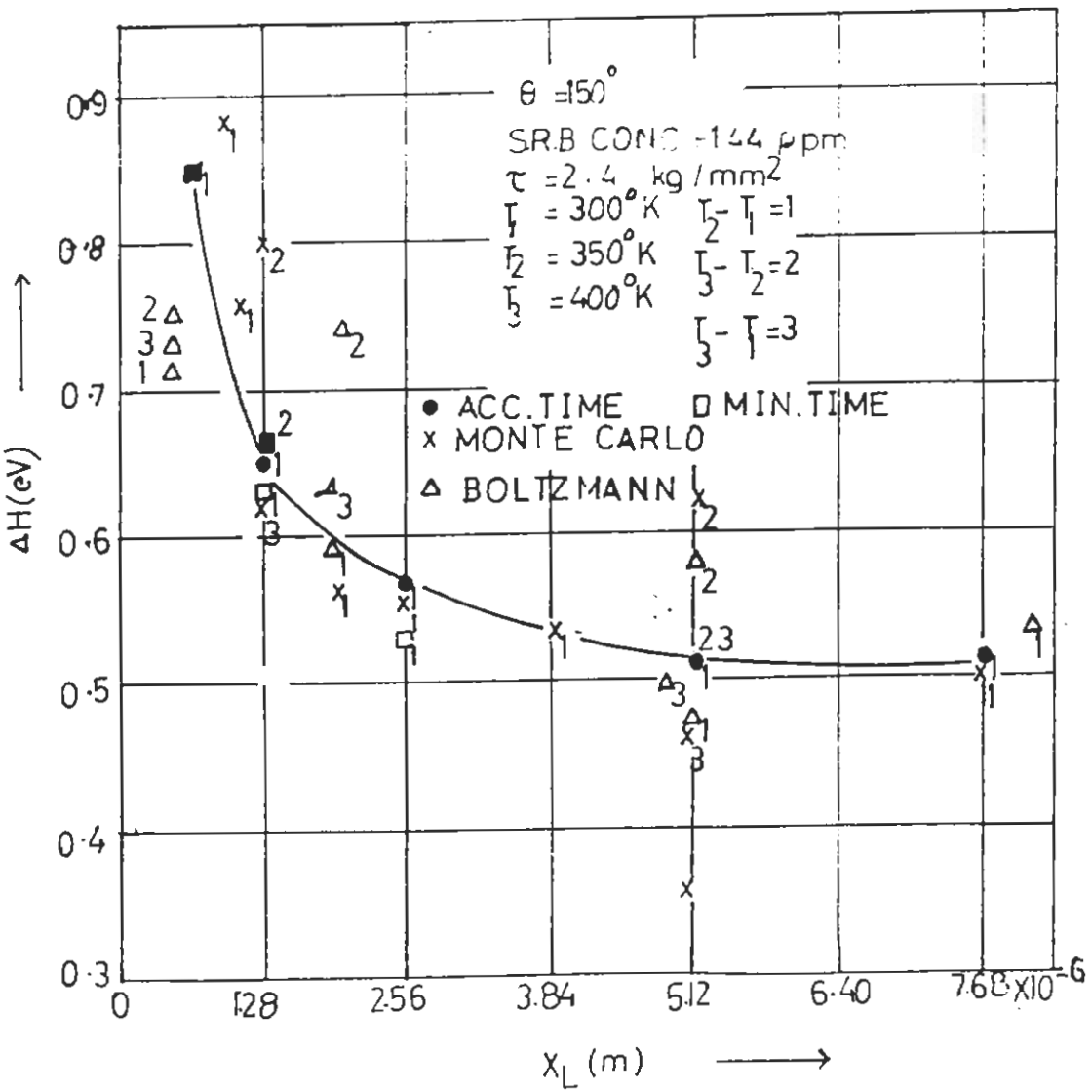

Fig. 17. The activation energy vs the width of the slip plane.

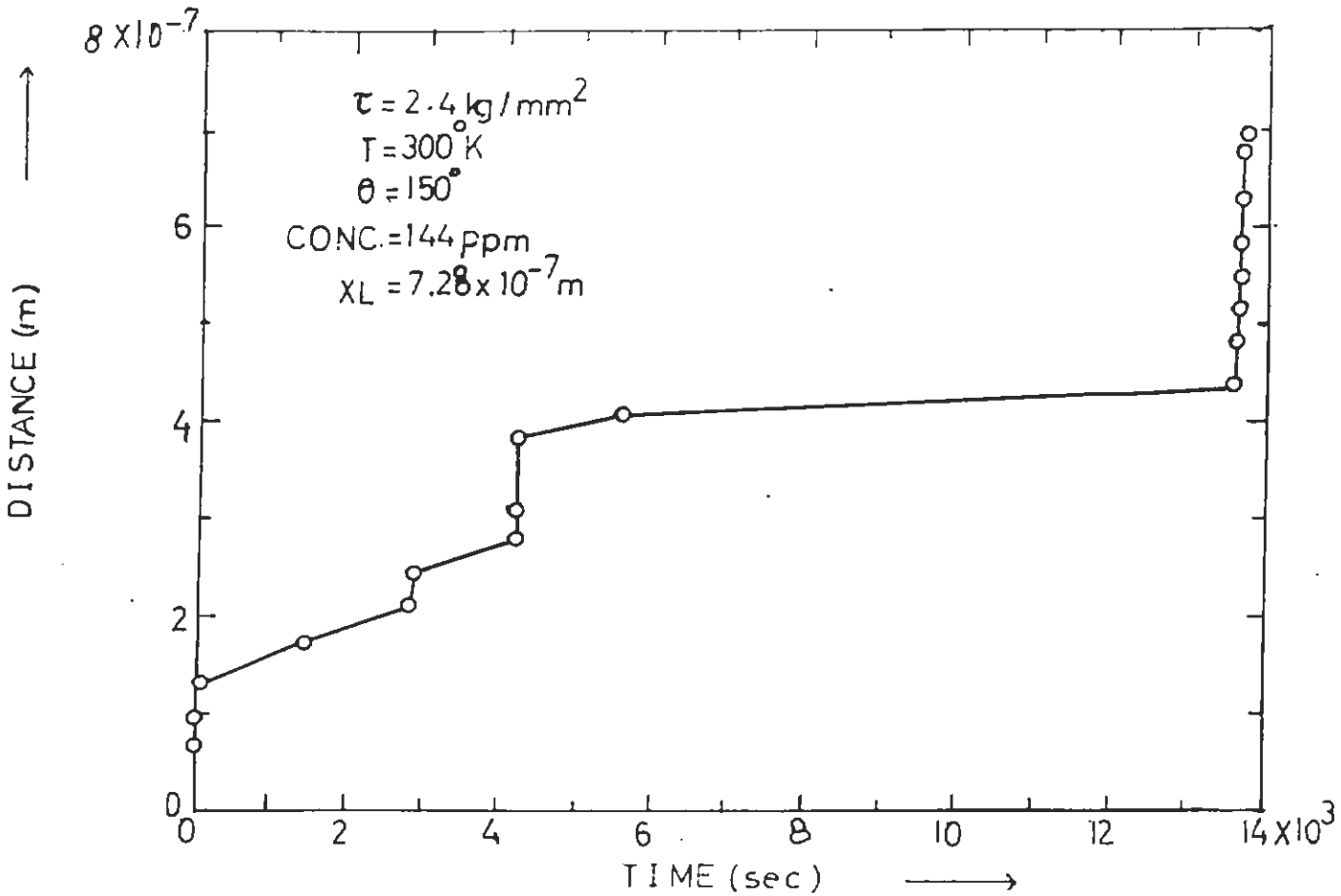

Fig. 18. (a) The distance traversed by a dislocation as a function of time.

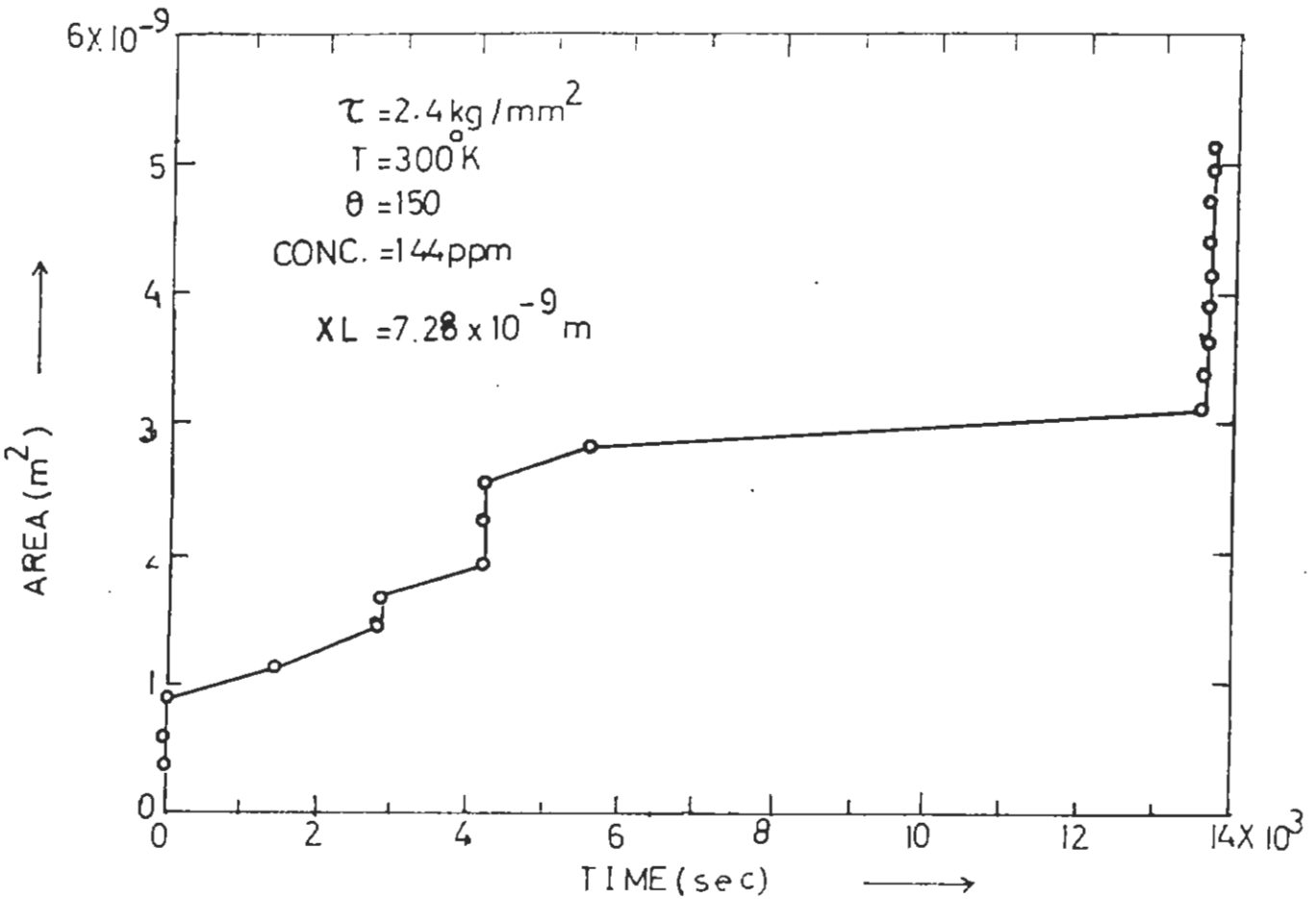

Fig. 18. (b) The area swept out by the dislocation as a function of time.

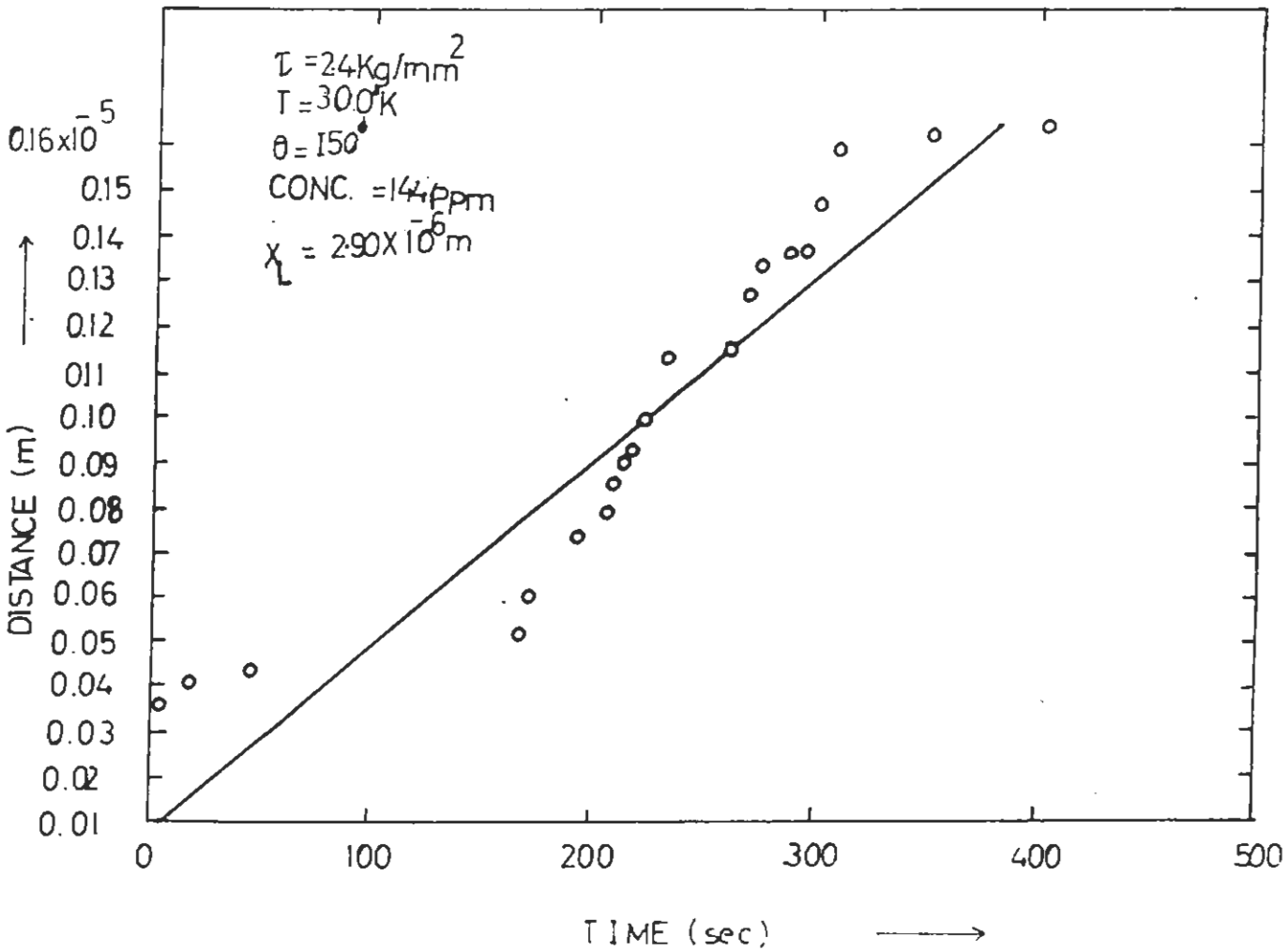

Fig. 19 . The distance traversed by the dislocation as a function of time.

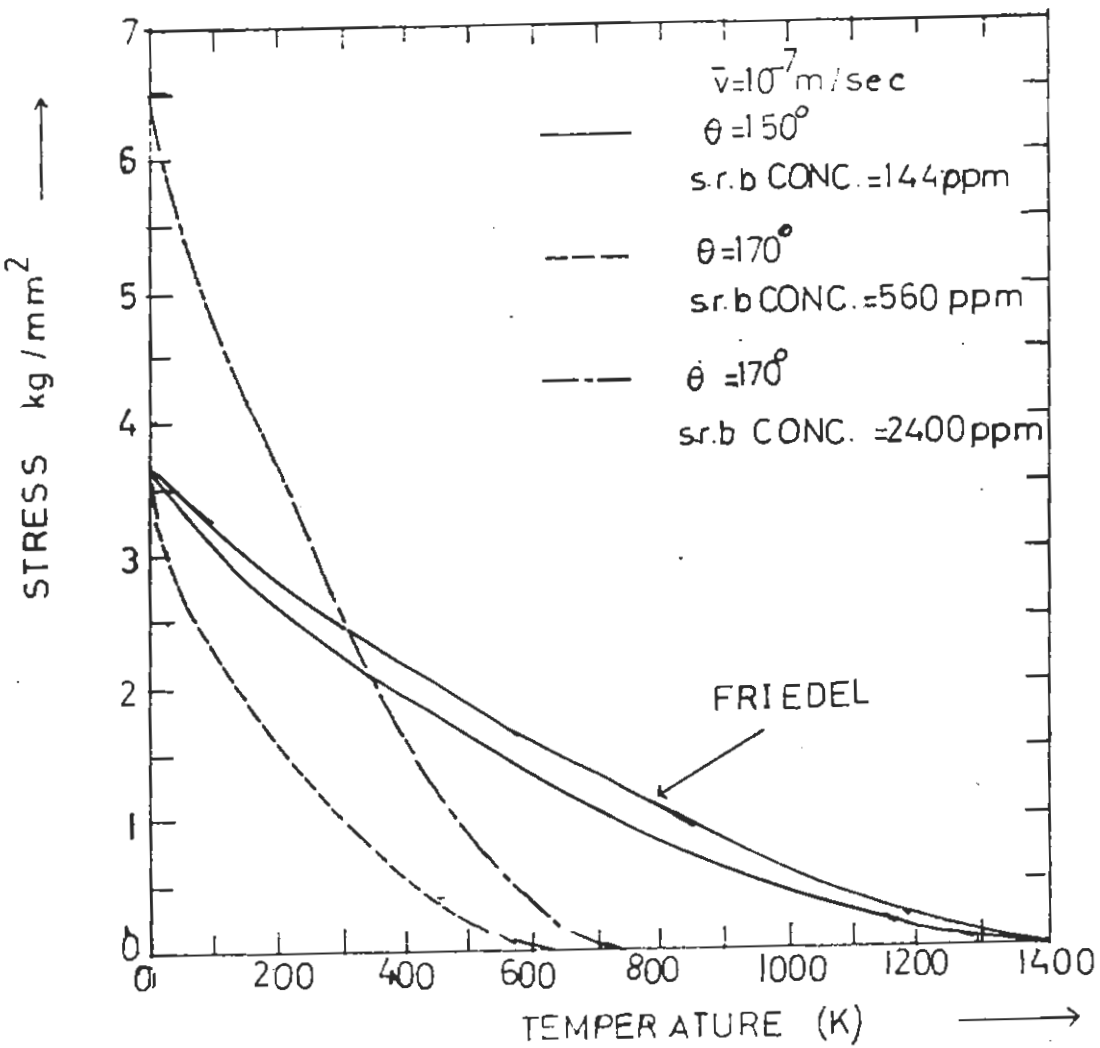

Fig. 20 · The stress required for a given dislocation velocity (10^{-7} m/sec) as a function of temperature.

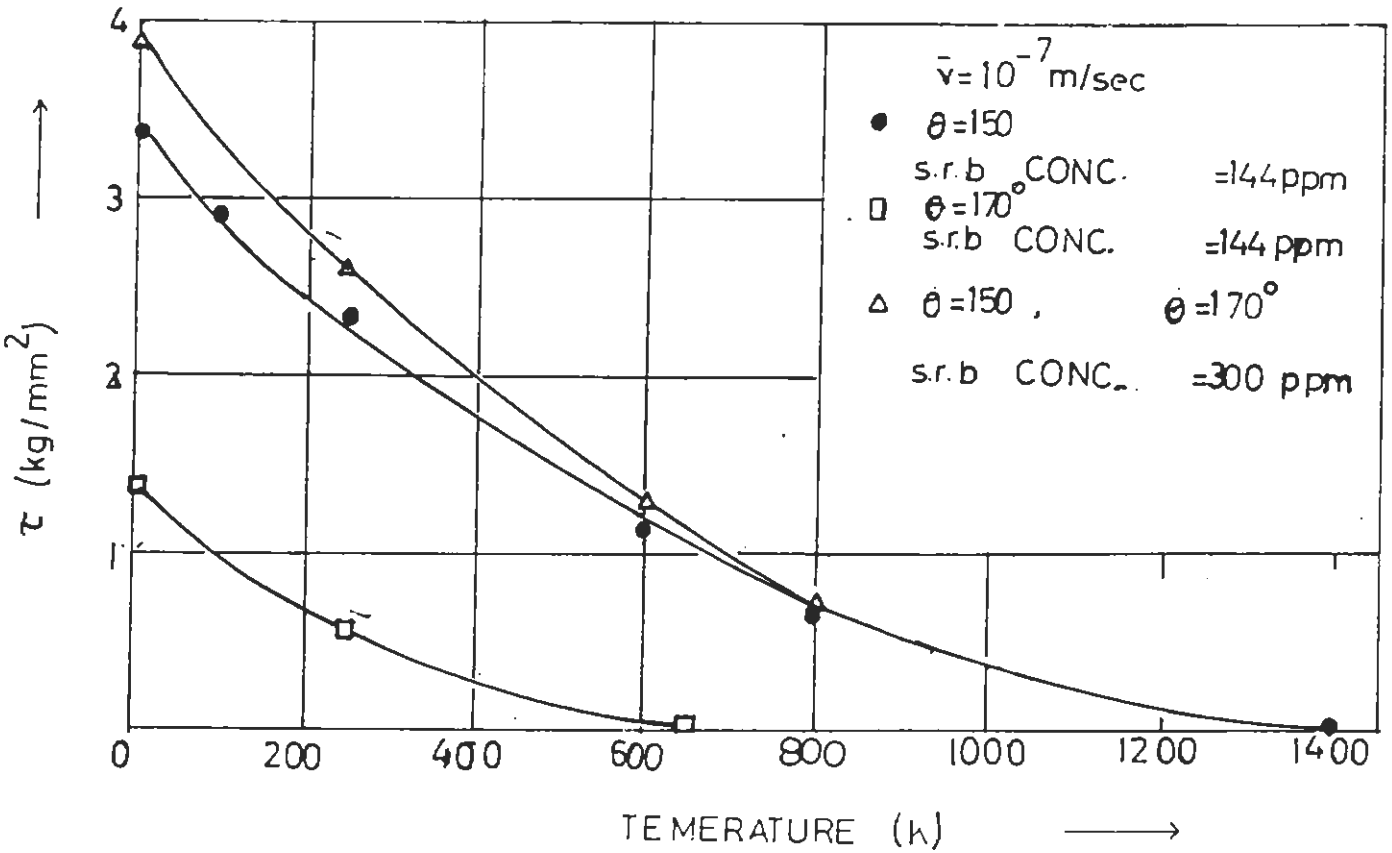

Fig. 21. The stress as a function of temperature at a given average dislocation velocity, where θ is a measure of the strength of the barriers.

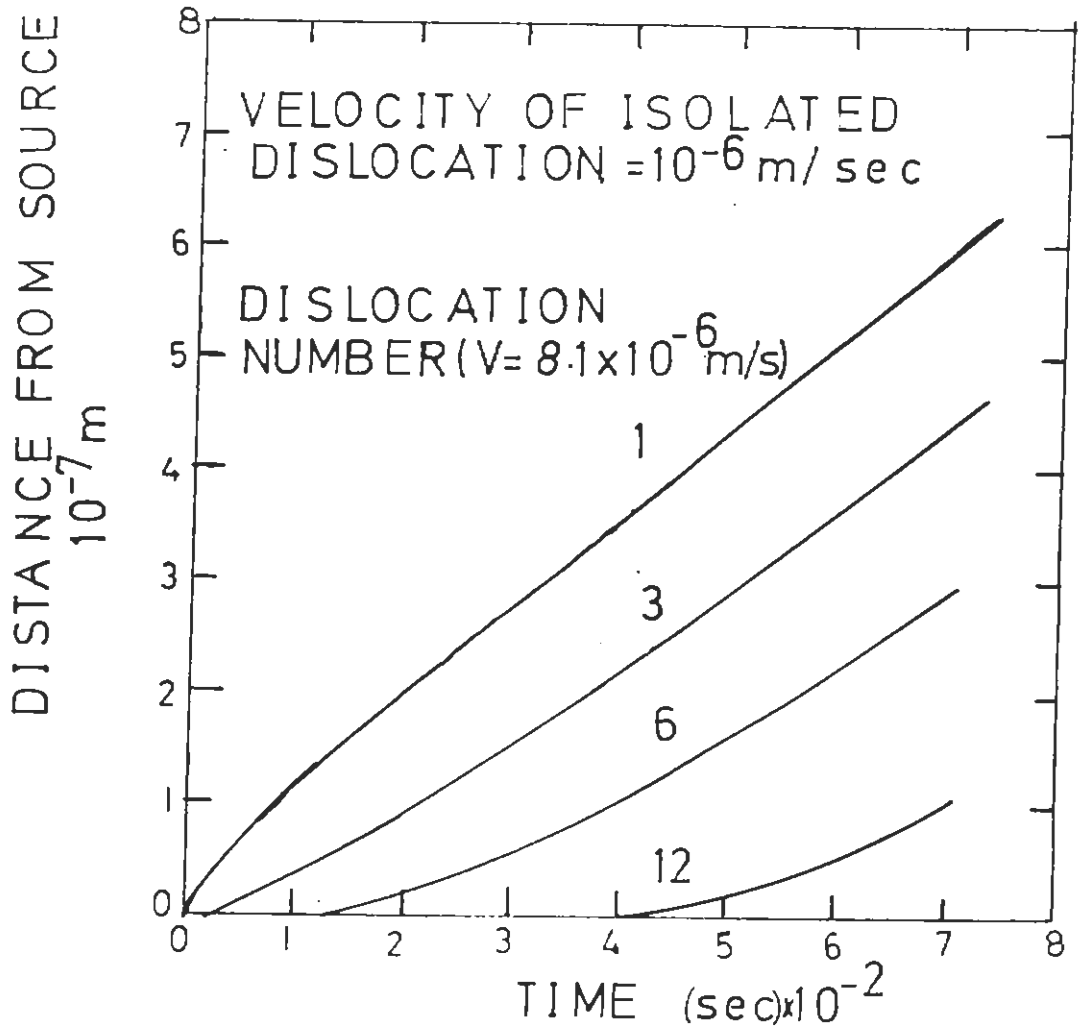

Fig. 22. Movement of some individual dislocations emitted by a source. A total of 20 dislocations was generated during the calculation (Ref.84).

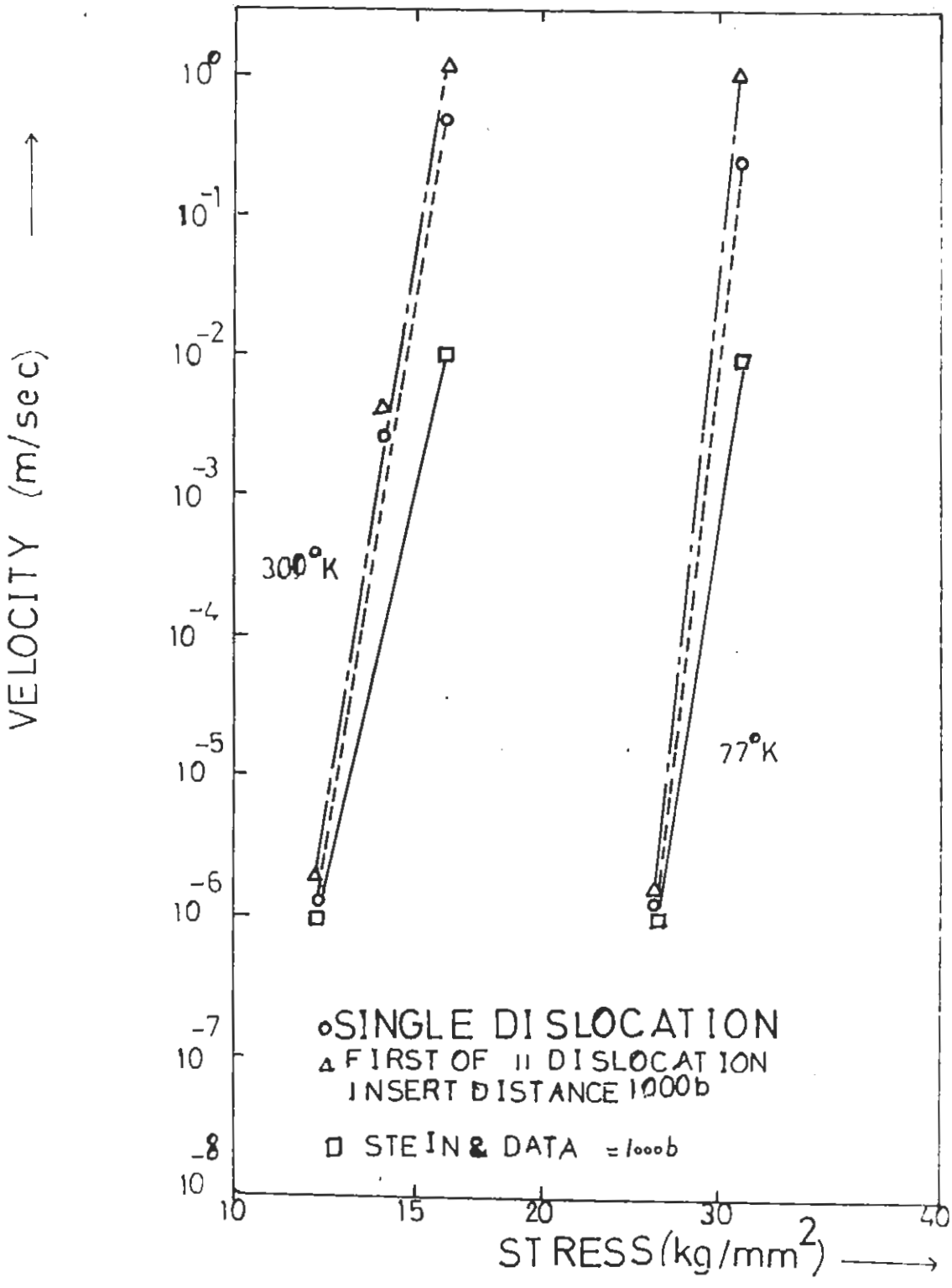

Fig. 23 . The steady velocity vs applied stress.

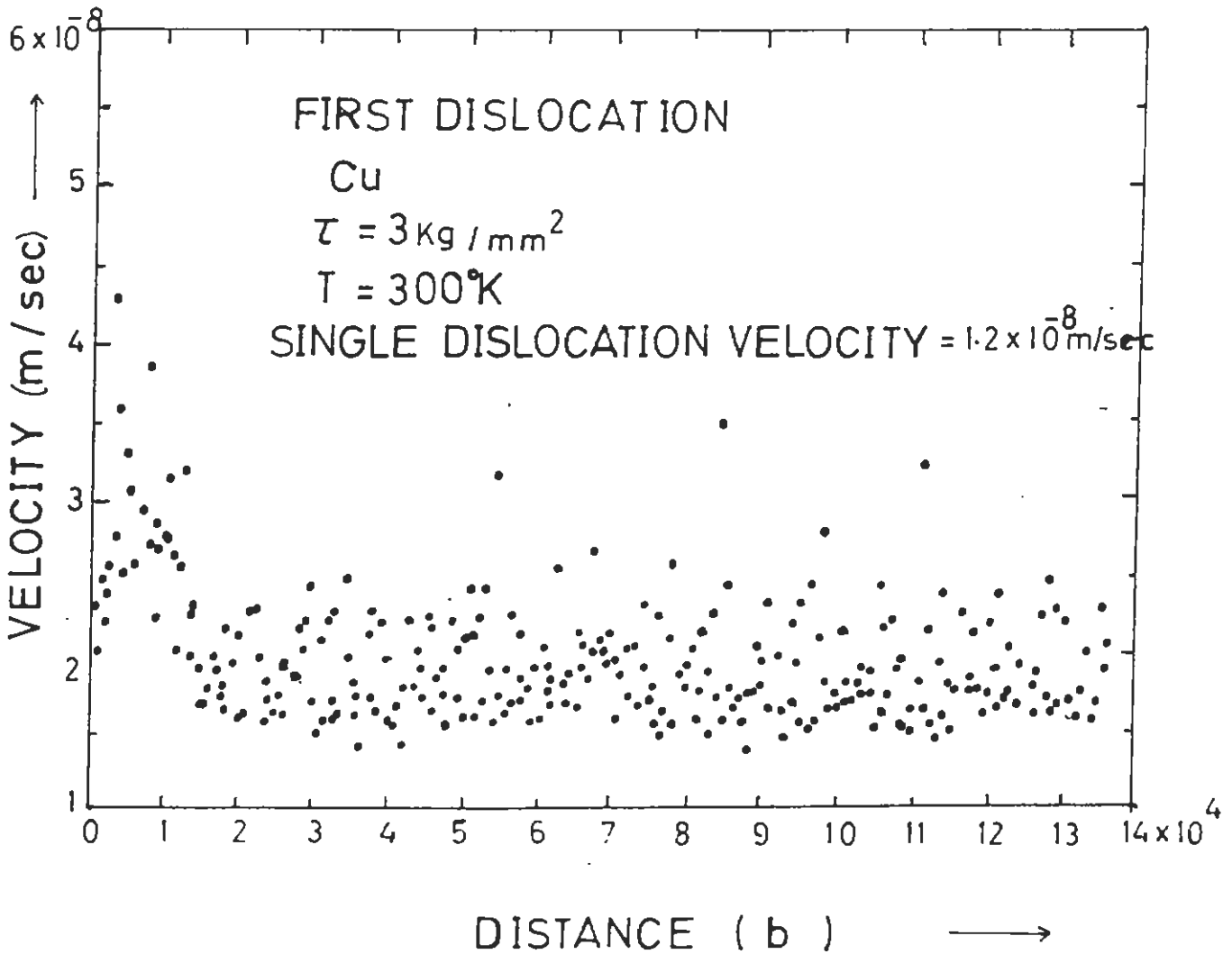

Fig. 24. The instantaneous velocity of the first dislocation as a function of distance from the source.

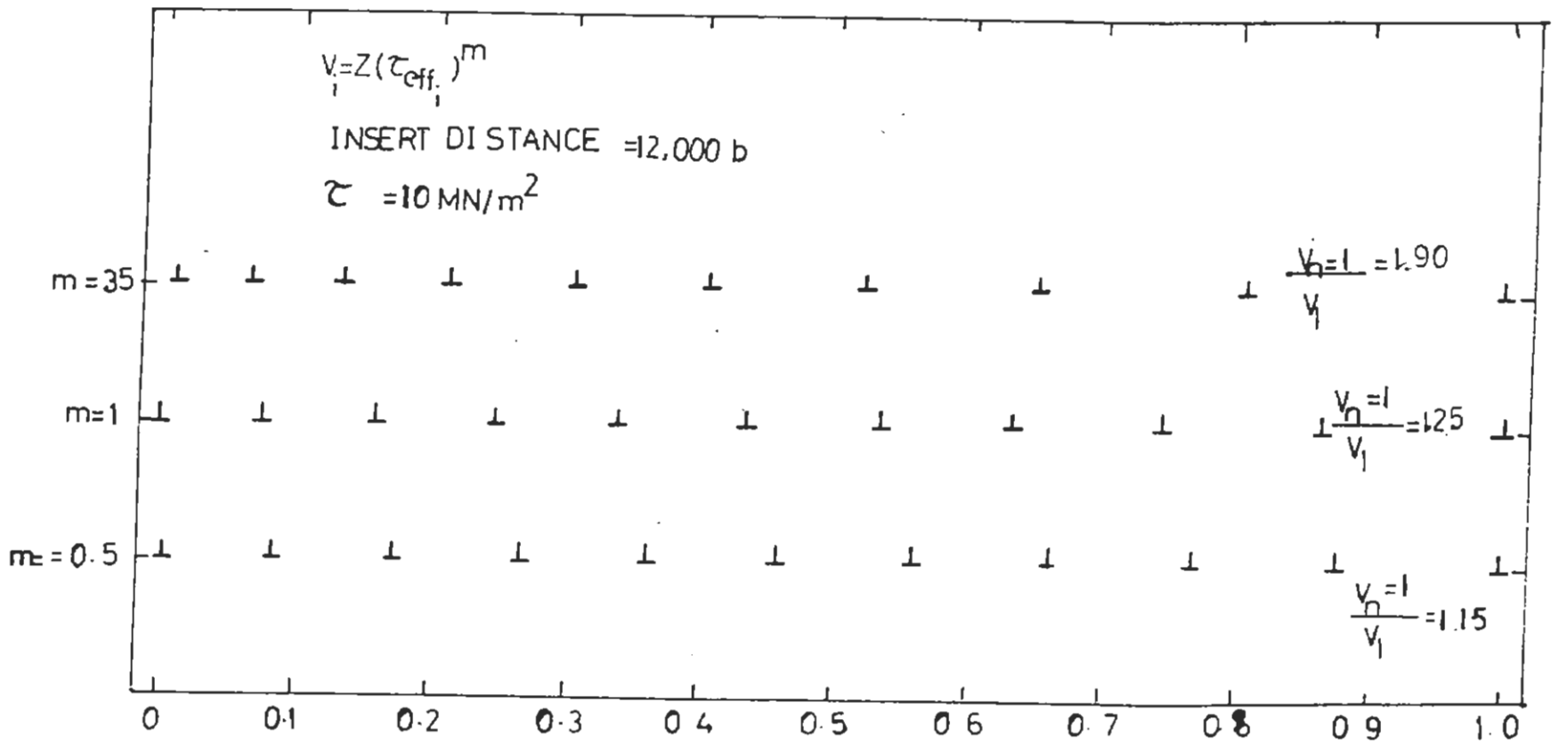

Fig. 25. (a) Dislocation configurations for various values of stress exponent.

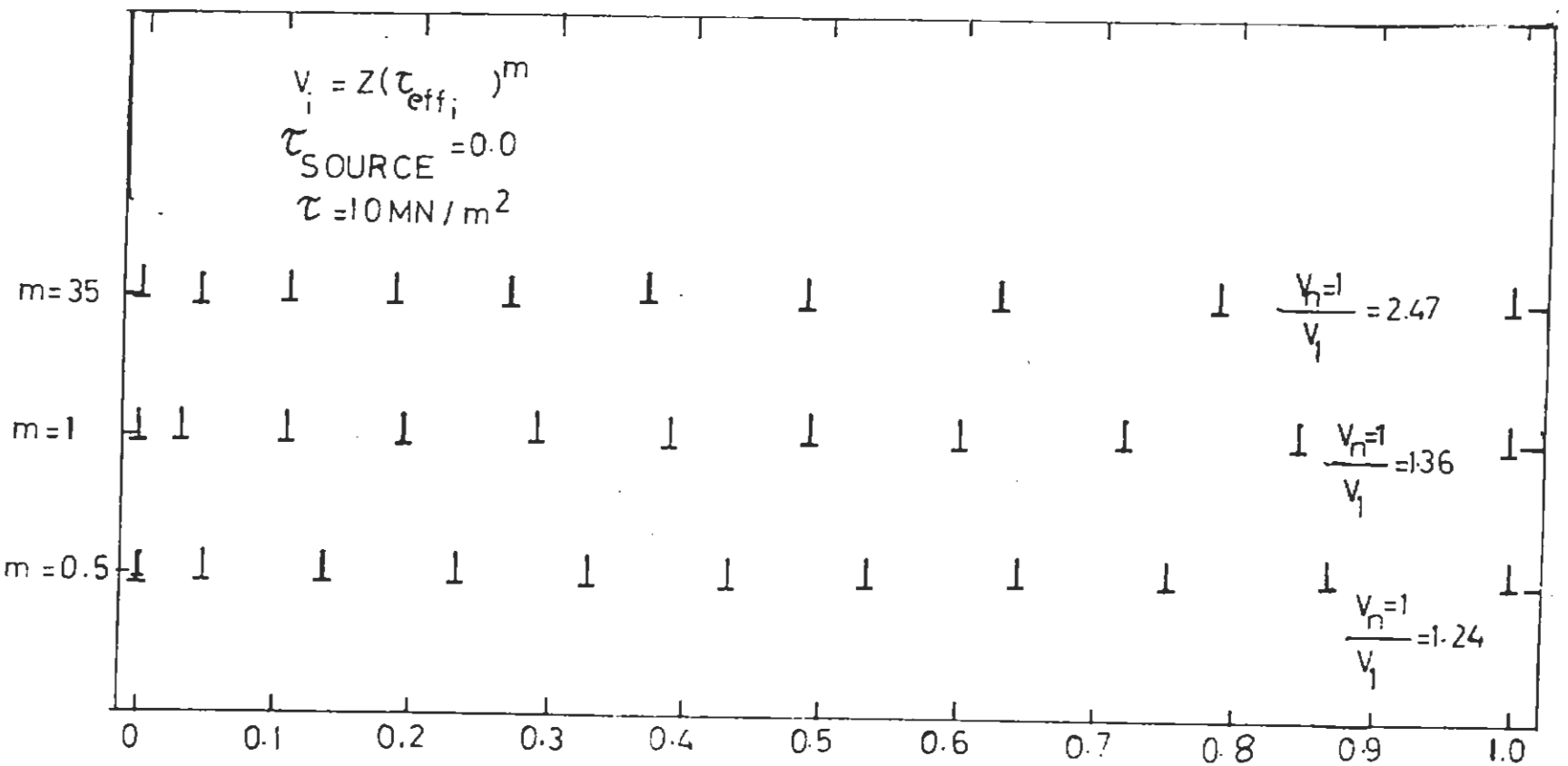

Fig. 25. (b) Dislocation configurations for various values of stress exponent.

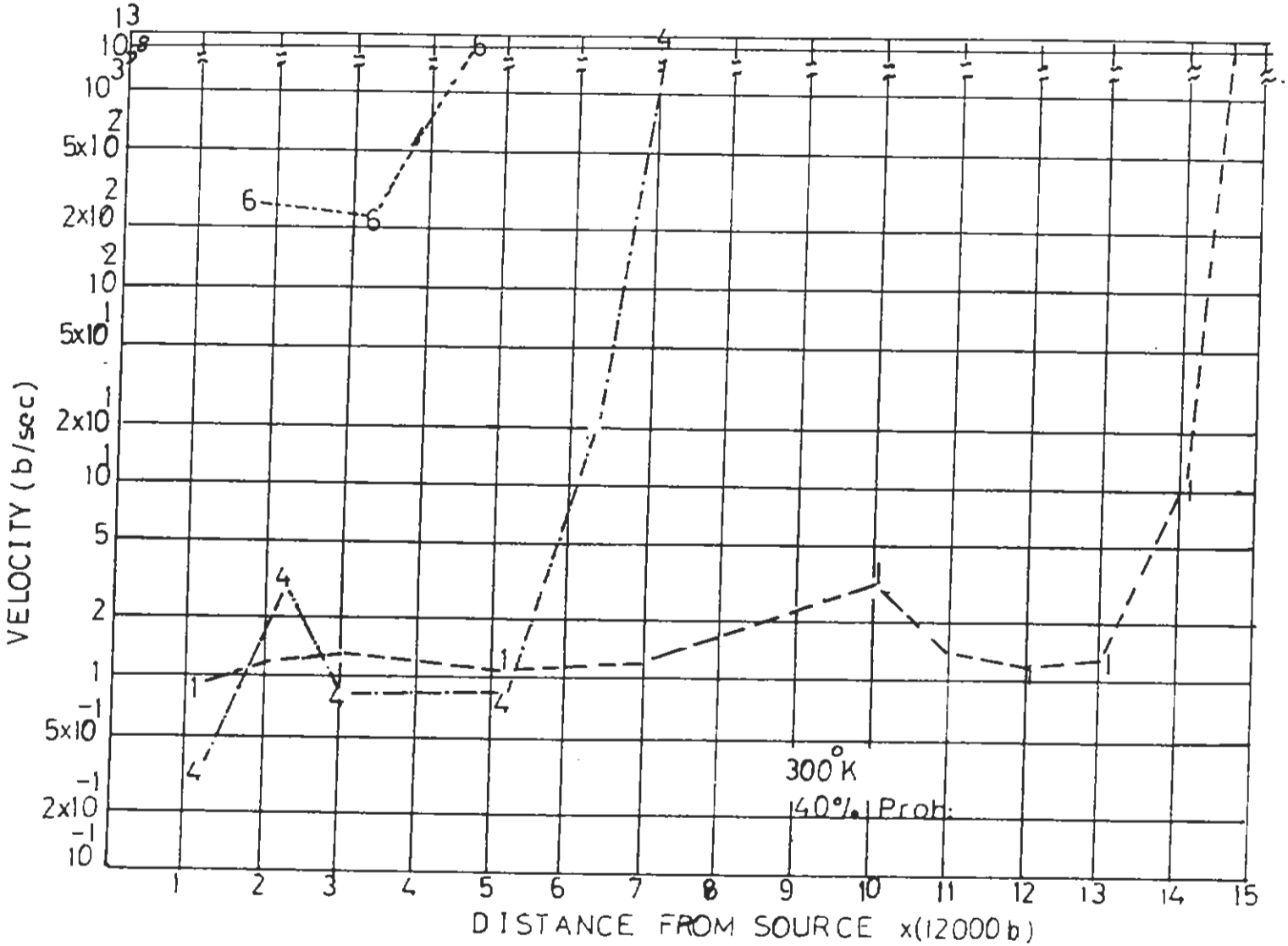

Fig. 26. The instantaneous velocity of the first 8 dislocations as a function of distance from the source.

REFERENCES

1. W.Meissner, M.Polanyi and E.Schmid, Z.Phys. 66(1930)477.
2. J.W.Glen, Phil. Mag.1 (1956)400.
3. O.H.Wyatt, Proc. Phys. Soc. 668 (1953)459.
4. F.Garofalo, Fundamentals of Creep and Creep-Rupture in Metals (Macmillan, New York, 1965).
5. N.Mott, Phil. Mag. 44 (1953)742.
6. J.Friedel, Dislocations (Pergamon Press, London, 1964).
7. A.Seegar, Z.Naturf. 9a (1954)758.
8. N.Mott, Phil. Mag. 1 (1956)568.
9. F.R.N.Nabarro, Theory of Crystal Dislocations, (Clarendon Press, Oxford, 1967).
10. G.Leibfried, in : Dislocations and Mechanical Properties of Crystals (Wiley, New York, 1957).
11. J.Weertman, J.Appl. Phys.29 (1958)1685.
12. G.Alefeld, Phys. Rev. Lett.2 (1964)372.
13. J.Gilman, J. Appl. Phys.39(1968)6086.
14. B.V.Peturhov and V.L. Pokrovskiĭ, Zh.Eksp. Teor. Fiz. Pisma 15 (1972)63 (in Russian); JETP Lett. (English Trans)15 (1972)44; Zh.Eksp. Teor. Fiz.63 (1972)634 (in Russian); Sov.Phys.JETP (English Trans)36 (1973)336.
15. V.D.Natsik, A.I. Osetskü, V.P.Soldatov and V.I.Startsev, Phys.Stat. Sol.(b)54 (1972)99.
16. V.D. Natsik, Fiz. Nizk. Temp.5 (1979)400 (in Russian); Sov.J.Low Temp. Phys. (English Trans)5, No.4 (1979)191.
17. R.P.Feynman and A.R.Hibbs, Quantum Mechanics and Path integrals (M cGraw-Hill, New York 1965).
18. P.Guyott and J.Dorn, Canad. J.Phys.45 (1967)983.
19. J.Hirth and J.Lothe, Theory of dislocations (McGraw-Hill, New York, 1968).
20. A.Granato and K. Lücke, J.Appl. Phys.27 (1956)583.
21. Taubert P.Abh. Dt. Akad. Wiss. Berl.: Kl.Math. Phys.Techn.1 (1958)58.
22. Feltham P.Phys. Stat. Solidi 30 (1968)135.
23. Landau AI. Phys. Stat. Solidi (a)15 (1973)343.
24. Tunaley JKE. J.app.Phys.43 (1972)4777.
25. Conrad H, Armstrong R,Wiedersich H and Schoek G.Phil Mag.6 (1961)177.
26. Bekirovic M, Feltham P and Michelson D.J.Mater.Sci (1974) in the Press.
27. Wyatt O H. Proc. Phys. Soc B 66 (1953)459.

28. Feltham P, Lehmann G and Moisel R. Acta Metall 17(1969)1305.

29. Rohde RW and Nordstrom TV. Scr. met 7 (1973)317.

30. P.Feltham, Rev.Def. Beh. Materials, 1 (1974)1.

31. B. Modeer and A.Oden, J.Mat Sci., 10(1975)223.

32. P.Feltham, J.Physics D (London),6 (1973)2048.

33. A.A.Maradudin; Interatomic Potentials and Simulation of Lattice defects, Edited by, Pierre C.Gehlen, Joe R.Beeler, Jr.Robert I.Jafee, Battelle Institute Materials Science Colloquia, Seattle, Washington, U.S.A., and Harrison Hot springs, B.C., Canada. June 14-19,(1971), Plenum Press New York - London (1972); pp.27.

34. J.H.Weiner and A.Askar; Interatomic Potentials and Simulation of Lattice defects, Edited, Pierre C.Gehlen, Joe R. Beeler, Jr. Robert I. Jafee, Battelle Institute Materials Science Colloquia, Seattle, Washington, U.S.A., and Harrison Hot Springs, B.C., Canada. June 14-19,(1971), Plenum Press New York - London (1972); pp.177.

35. P.S.HO; Ibid. pp.321. (36)R.Chang, Ibid. pp.391. (37)J.R.Parsons, Ibid pp.463. (38)P.C.Gehlen, Ibid. pp.475. (39)V.Vitek, L.Lejcek and D.K. Bowen, Ibid.pp.493. (40)R.C.Perrin, A.Englert, and R.Bullough, Ibid.pp.509. (41)Z.S.Basinski, M.S.Duesbery and R.Taylor, Ibid.pp.526. (42)Z.C.Basinski, M.S.Duesbery and R.Taylor, Ibid.pp.537. (43)W.R.Taylor, Ibid.pp.553. (44)D.P.Jackson, Ibid.pp.621. (45)F.W.de Wette . Ibid.pp.653. (46)R.E.Dahl,JR.,Jr.Beeler, and R.D. Bourquin, Ibid.pp.653. (47)M.J.Weins, Ibid.pp.695.

48. Bullough, R., Perrin, R.C., Proc. R.Soc. A 305 (1968) 541.

49. Perrin, R.C., Englert, A., Bullough, R., Interatomic Potentials and Simulation of Lattic defects (Beeler, J.R., Gehlen, P.C., Eds), Battelle Colloq., Harrison Hot Springs, B.C. (1971).

50. N.Farooqui, S.M.Raza, S.M.Nasir, Stochastic Model of Low Temperature Creep., presented in the Third Asia Pacific Physics Conference, Hong Kong, 20-24 June,(1988).

51. P.Feltham, J.Phys. D(London 6, 2048(1973).

52. V.A.Buckle and P.Feltham, Metals, Science 9, 541 (1975).

53. S.M.Raza, Scripta Metall. 16, 1325 (1982).

54. S.M.Raza, S.B.H.Abidi and N.Farooqui, Appl. Phys. Lett.46 (1), 34 (1985).

55. H.Mughrab and U.Essman, in Strength of Metals and Alloys, edited by P.Hassen (Pergamon, Oxford & New York, (1979).

56. P.Feltham, Freiberger Forschungshefte, B 109, 29 (1965).

57. K.K.Ray and A.K. Malik, Mater. Sci. Eng. 59, 59 (1983).

58. V.I.Dotsenko and A.I.Landaue, Mater. Sci Eng. 22, 101(1976).

59. S.M.Raza and M.Z.Butt, J.Mater Sci. letts.3, 629 (1984).

60. S.M.Raza and M.Z.Butt, J.Mater Sci. letts.3, 955 (1984).

61. S.M.Raza, J. Appl.Phys. 55, 296 (1984).

62. S.M.Raza, Acta Metall. 33, 1285 (1985).

63. S.M.Raza, N.Farooqui, S.B.H.Abidi, and A.K. Khan Fizika 16, 357 (1984).

64. S.M.Raza and S.A.Raza, J.Mater. Sci letts. 5, 25 (1986).

65. S.M.Raza, Nucleus 22, 15 (1985).

66. M.Hamersky and Z.Trojanova, Czech, J.Phys. B.35, 292(1985).

67. S.M.Raza, N.Farooqui et al, Phys. Stat. Sol.(a)100, K149 (1987).

68. A.J.E.Foreman and M.J. Makin, Cand. J. of Phys., 45, 511 (1967).

69. U.F.Kocks, Can. J.Phys., 45, 737 (1967).

70. K.Hanson and J.W. Morris, Jr., J.Appl. Phys., 46, 983(1975).

71. R.Scattergood and E.S.P. Das, Proceedings of the Conference on Computer Simulation for Materials Applications, Ed. by R.J.Arsena ult, J.B. Beeler, and J.A.Simmons., 1976, p.740.

72. T.J. Koppenaal and D.K.Wilsdorf, Appl. Phys. Letters, 4, 59 (1964).

73. H.J.Frost and M.F.Ashby, J.Appl. Phys., 42, 5273(1971).

74. W.Rose, Introduction to Statistics. (Plenum Press 1979).

75. D.Klahn, D.Austin, A.K., Makharjee and J.E.Dorn, Proceedings of the Symposium on Statistical and Probabilistic Problems in Metallurgy, Special Supplement to Advances in Applied Probability, DEc. 1972, p. 112.

76. R.J.Arsenault and T.W. Cadman, Rate Processes in Deformation of Materials, ASM Publisher, 1975, p.102.

77. R.J.Arsenault and T.W. Cadman, Scripta Metl, 7, 631 (1973).

78. J.W.Morris, Fr. and D.H.Klan, J.Appl. Phys.,45, 2027(1974).

79. P.Wynblatt, Rate Process in Plastic Deformation, A.S.M. Publisher, 1975, p.156.

80. R.J.Arsenault and T.W. Cadman, Proceedings of the Conference on Computer Simulation for Materials Applications, Ed. by R.J.Arsenault, J.B. Beeler, and J.A.Simmons, 1976, p.658.

81. T.W. Cadman and R.J. Arsenault, Scripta Met., 6, 593(1972).

82. K.Hanson S.Altintas and J.W.Morris, Proceedings of the Conference on Computer Simulation for Materials Applications, Ed. by R.J.Arsenault, J.B.Beeler and J.A.Simmons, 1976, p.917.

83. J.Friedel, Dislocations, Addison-Wesley, Reading, Mass., 1964, p.224.

84. R.J.Arsenault and T.W.Cadman, Phys. Stat. Sol., 24, 299 (1974).

85. A.R.Rosenfield and G.T.Hahan, Dislocation Dynamics, ed. by A.R. Rosenfield, G.T. Hahan, A.L.Bement and R.I.Jaffee, McGraw-Hill, New York, 1968, p.255.

86. R.J. Arsenault, T.Skrovaneck and T.W. Cadman, to be published.

87. D. Stein and J.Low, J.Appl. Physics., 31, 362 (1960).

88. R.J. Arsenault, Phil. Mag., 24, 259 (1970).

89. N.Farooqui, D.Carr and S.M.Raza "Time Dependent Solution for Dislocation Shape as a Function of Breaking Angle". submitted in Computational Physics (1990).

90. N.Farooqui and S.M.Raza, "Simulation of Dislocation Motion and Average Velocity". submitted in J.Phys. F.(1990).